



a Payload for Antimatter Matter Exploration
and Light-nuclei Astrophysics



Studies of positron identification with the PAMELA calorimeter

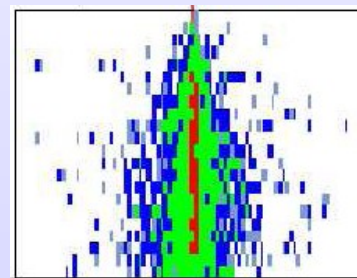
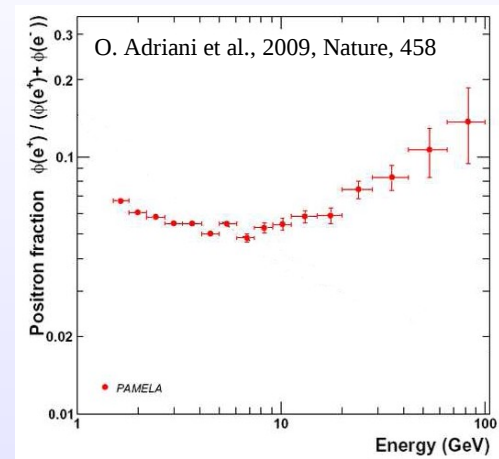
Laura Rossetto

Licentiate seminar, November 10th 2010, Stockholm

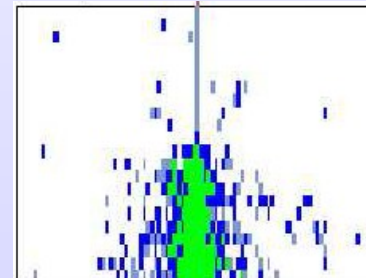


Outline

- **Basic concepts of cosmic rays**
 - acceleration and propagation mechanisms
 - solar modulation
 - cosmic ray positrons and the PAMELA positron fraction
- **The PAMELA experiment**
 - description of the components
- **Shower development in the PAMELA calorimeter**
 - description of electromagnetic and hadronic shower development inside the calorimeter
 - π^0 contamination of hadronic showers
- **Simulation studies of π^0 contamination**
 - the “Nature analysis” approach applied to simulations
 - a new approach for positron identification



electromagnetic
cascade

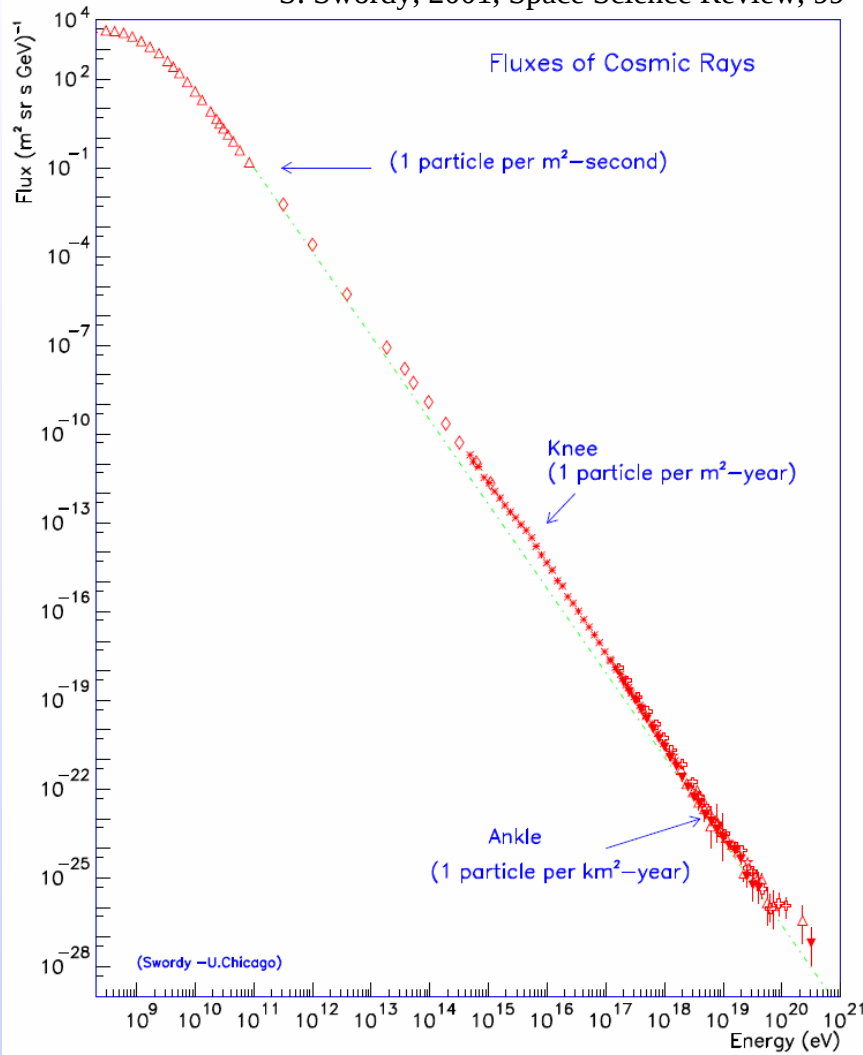


hadronic
cascade



Cosmic rays

S. Swordy, 2001, Space Science Review, 99



- Cosmic rays:
 - ~ 98% protons and nuclei
 - ~ 2% electrons
- all particle energy spectrum follows a power-law distribution $E^{-\alpha}$
 - for $E > 10^9$ eV, $\alpha = 2.7$
 - **knee** at $E \sim 3 \cdot 10^{15}$ eV, $\alpha = 3.1$
 - **ankle** at $E \sim 10^{18}$ eV, $\alpha = 2.7$
- for $E \leq 10$ GeV
 - solar modulation effect
- **primary** elements are accelerated in sources of high energy particles
- **secondary** elements are produced by spallation processes

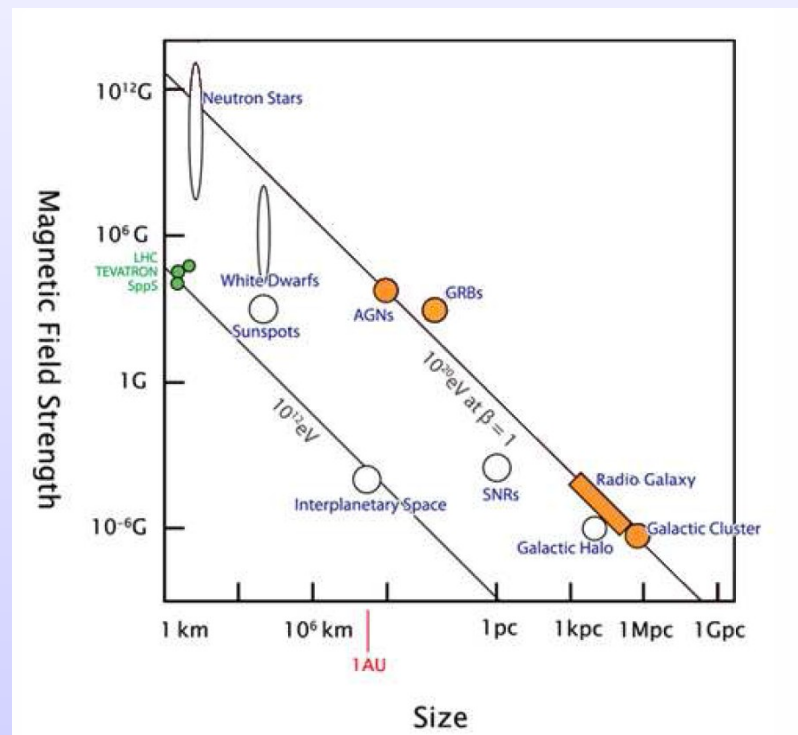


Acceleration mechanisms

- First order Fermi acceleration (1949) $\rightarrow \langle \Delta E / E \rangle = (2 / 3) \cdot (V / c)$
 - \rightarrow acceleration in strong shock waves, e.g. **supernovae explosions**
 - \rightarrow a power-law energy spectrum is obtained
 - \rightarrow acceleration phase $\sim 10^5$ years \rightarrow upper limit $E \sim 10^{14}$ eV
 - \rightarrow acceleration to higher energies \rightarrow pulsar magnetosphere, AGN, GRB...



Crab nebula

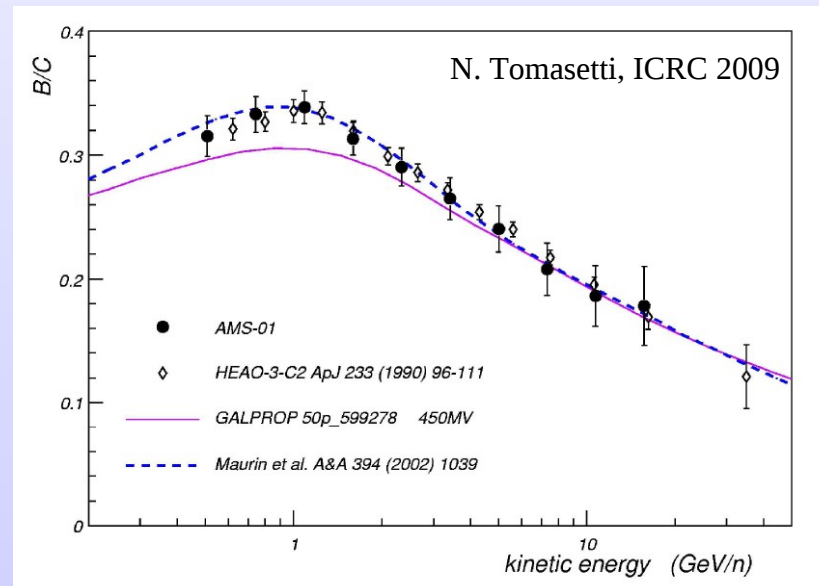


<http://jemeuso.riken.jp/en/about2.html>



Propagation mechanisms

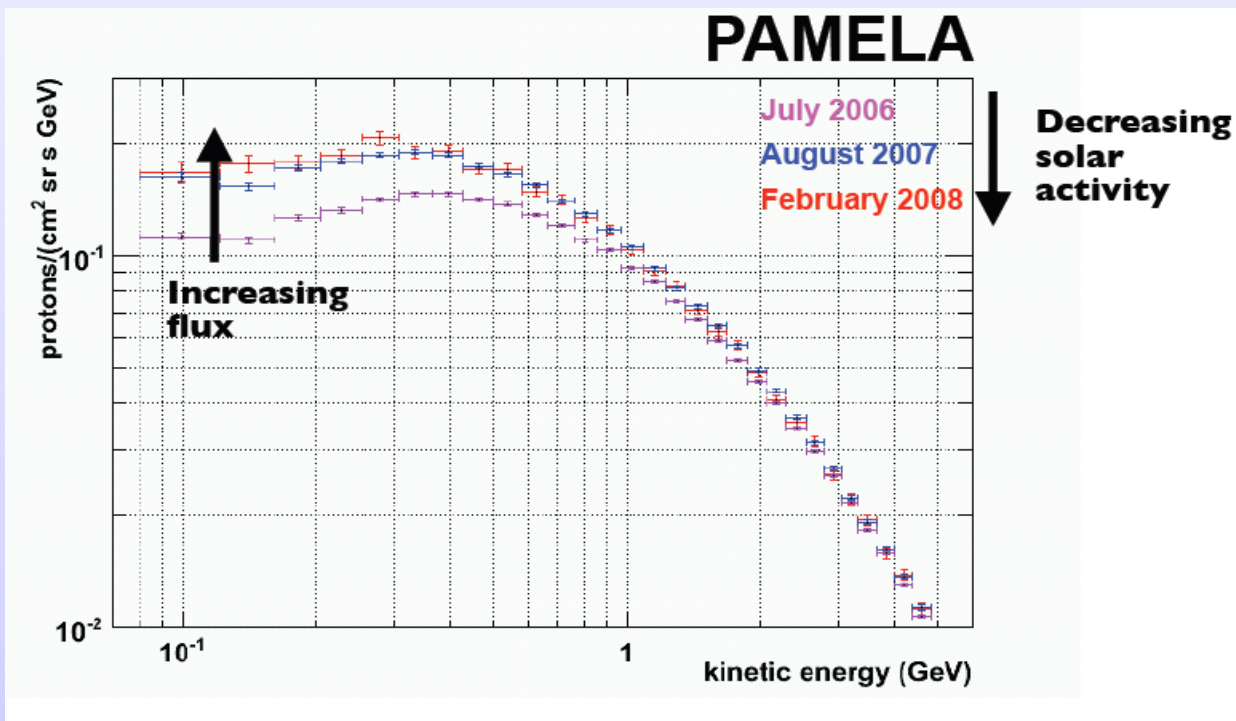
- Cosmic rays propagate through the interstellar medium losing energy
- the processes which participate in the particles transportation are
 - **diffusion**: it depends upon the particle density and the diffusion coefficient
 - **convection**: galactic winds of charged particles
 - **reacceleration**: inhomogeneities in the galactic magnetic field (Alfvén velocity)





Solar modulation

- Energy spectra of cosmic rays with $E < 10$ GeV are modified by the solar wind
- the intensity of the solar activity is periodic with a **11-year cycle**
- at each maximum the polarity of the solar magnetic field reverses
→ **22-year cycle**
- at the solar maximum → the flux of low energy particles is minimum





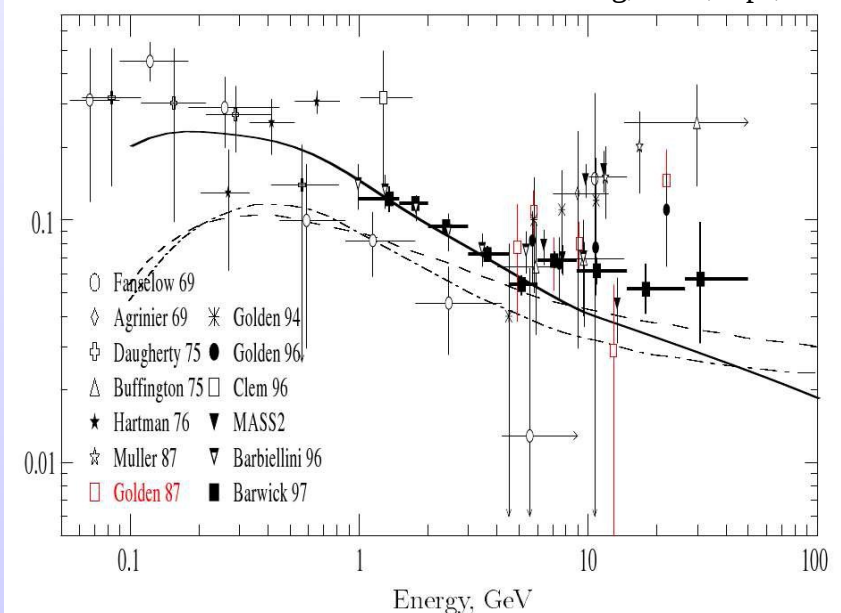
Cosmic ray positrons

- electrons account for $\sim 2\%$ of the cosmic ray particles
- proton-to-positron flux ratio is $\sim 10^4$ at 100 GV
 \rightarrow positrons can probe acceleration and propagation mechanisms in a galactic region of ~ 1 kpc (synchrotron radiation, inverse Compton scattering)
- positrons are believed to be mainly secondary particles: $p + p \rightarrow \pi^\pm, K^\pm$

$$\pi^\pm \rightarrow \mu^\pm + \nu_\mu \rightarrow e^\pm + \nu_e$$

$$K^\pm \rightarrow \mu^\pm + \nu_\mu, \pi^0 + \pi^\pm$$

$e^+/(e^+ + e^-)$ I.V. Moskalenko & A.W. Strong, 1998, ApJ, 493



— pure secondary production
without reacceleration

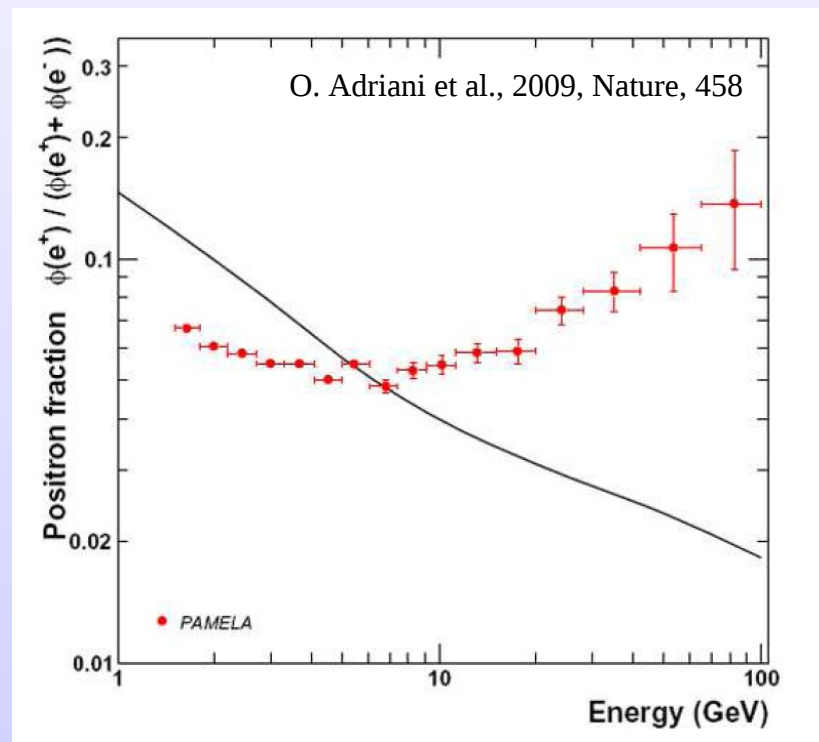
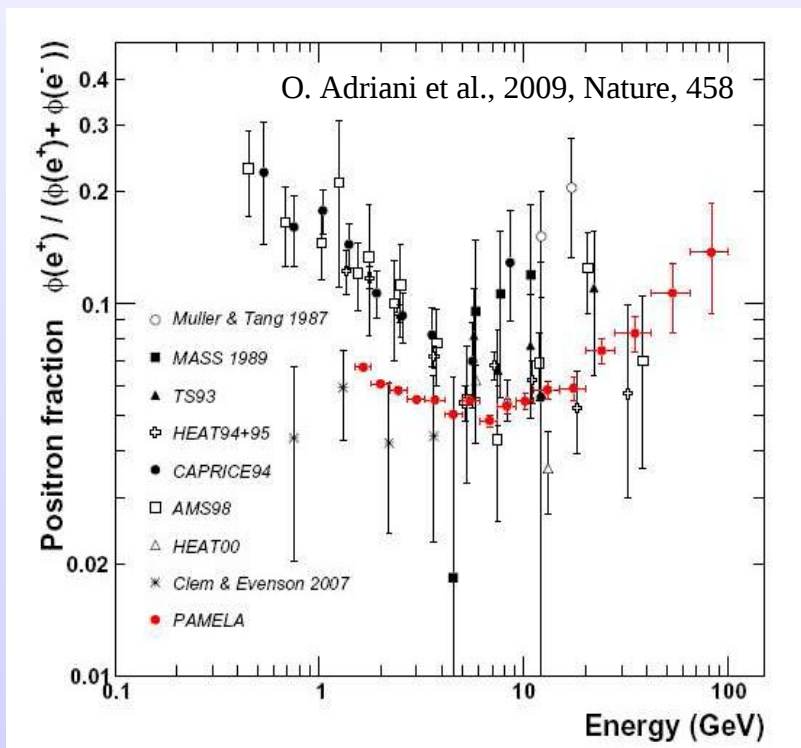
- · - leaky-box model

-- diffusion model



PAMELA positron fraction

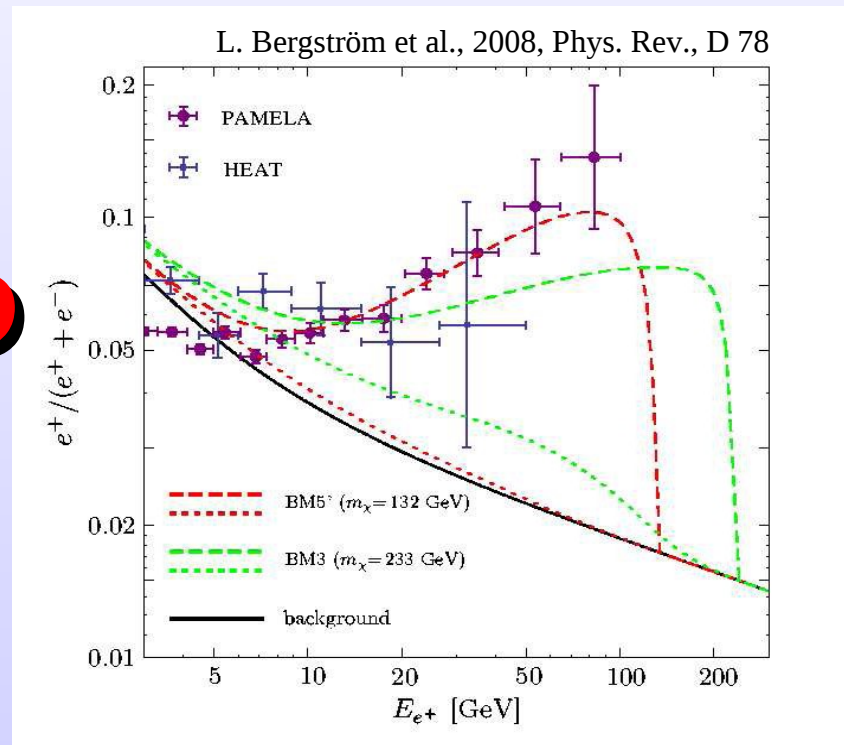
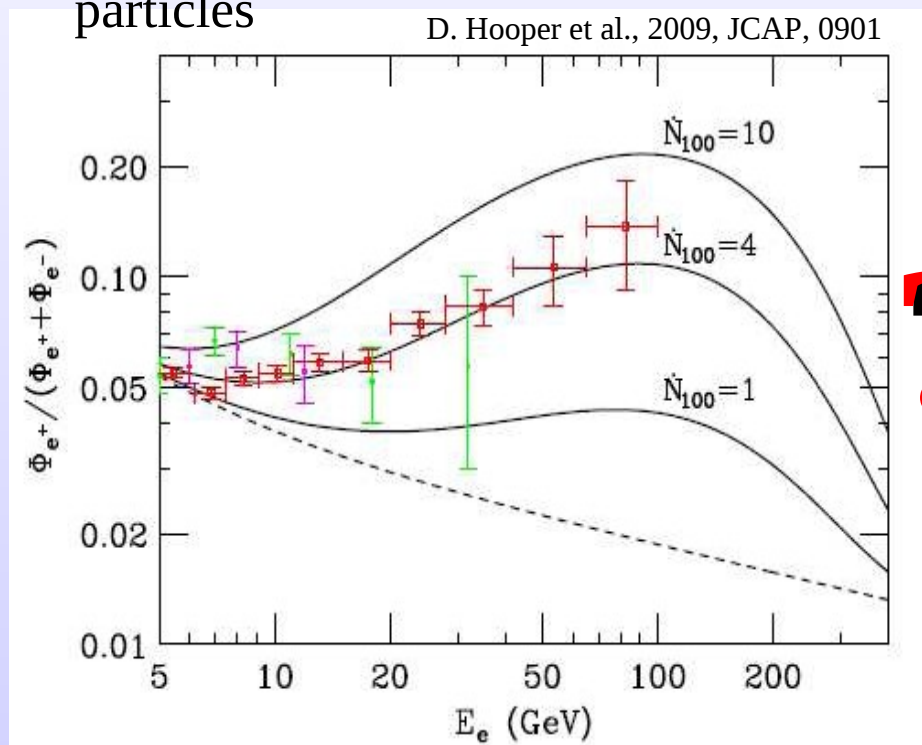
- Positron fraction measured between **1.5** and **100 GeV**
- result based on the data collected between July 2006 and February 2008
→ $\sim 10^9$ triggers, total acquisition time of ~ 500 days
- published in the journal Nature → widely discussed, more than **600 citations!**





PAMELA positron fraction

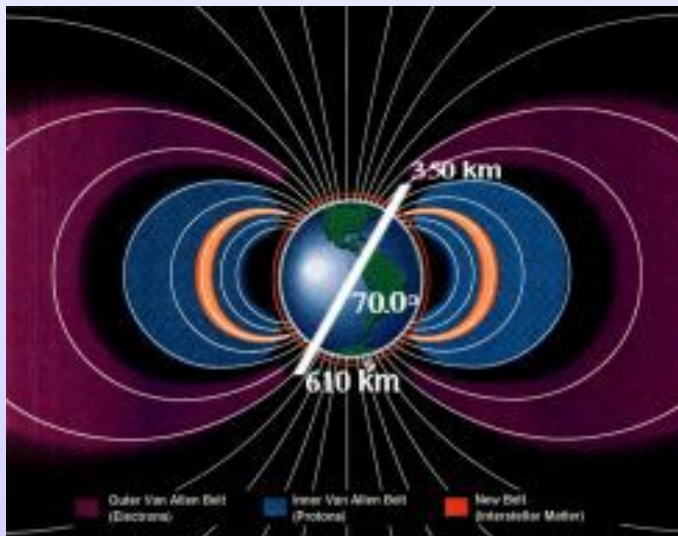
- Widely discussed → what is the reason to the rise at high energies?
- **Possible answers:**
 - pulsar magnetosphere could be source of primary cosmic ray positrons
 - primary positrons could be produced via annihilation of dark matter particles



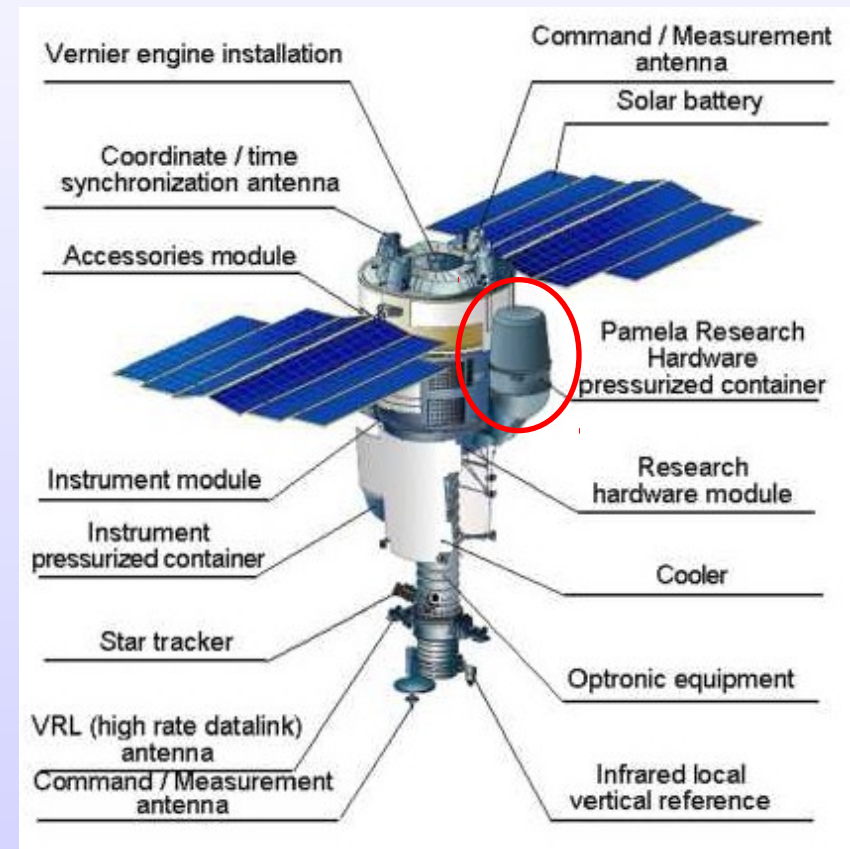


The PAMELA experiment

- PAMELA is mounted on board of the Russian Resurs DK1 satellite
- the satellite was launched from the Baikonur cosmodrome in Kazakhstan on **June 15th 2006**
 - elliptical and semi-polar orbit
 - altitude between **350 – 600 km**
 - inclination angle of **70°**



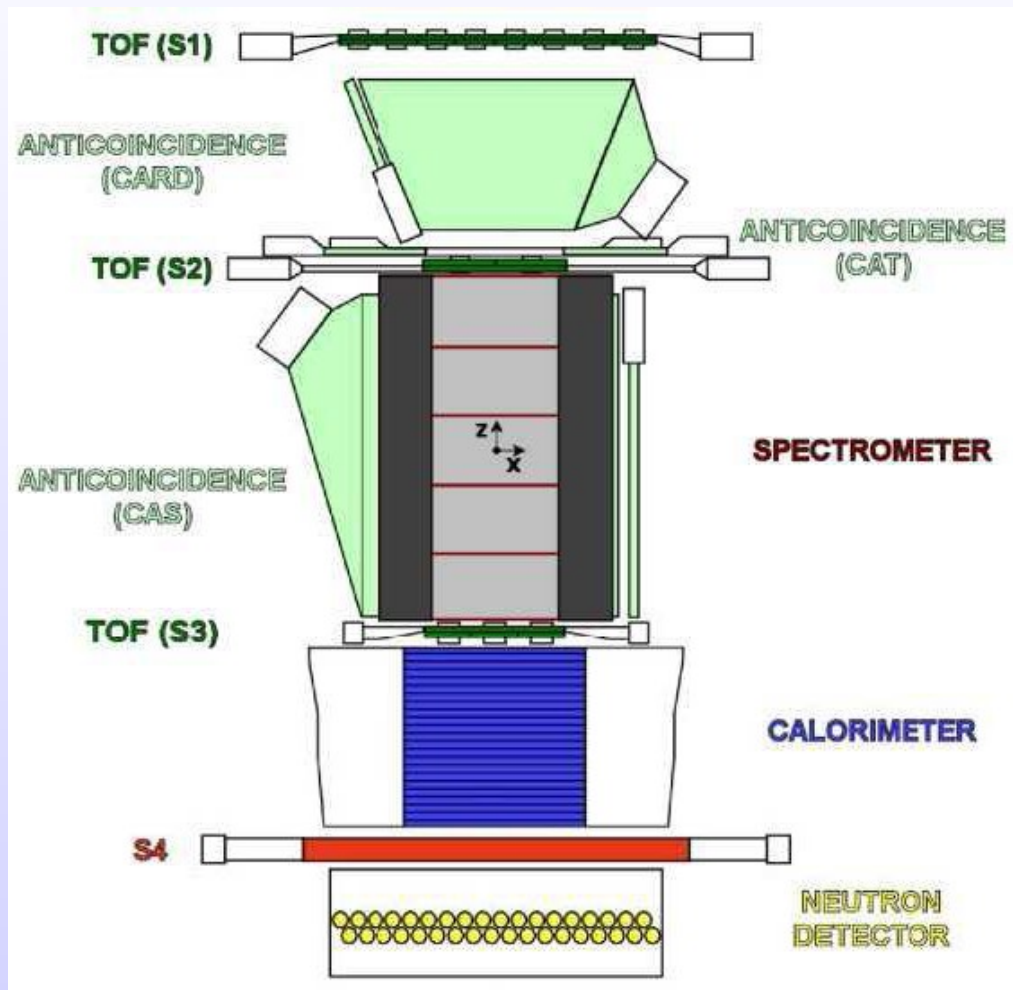
<http://pamela.roma2.infn.it>



P. Picozza et al., 2007, Astrop. Phys., 27



The PAMELA experiment

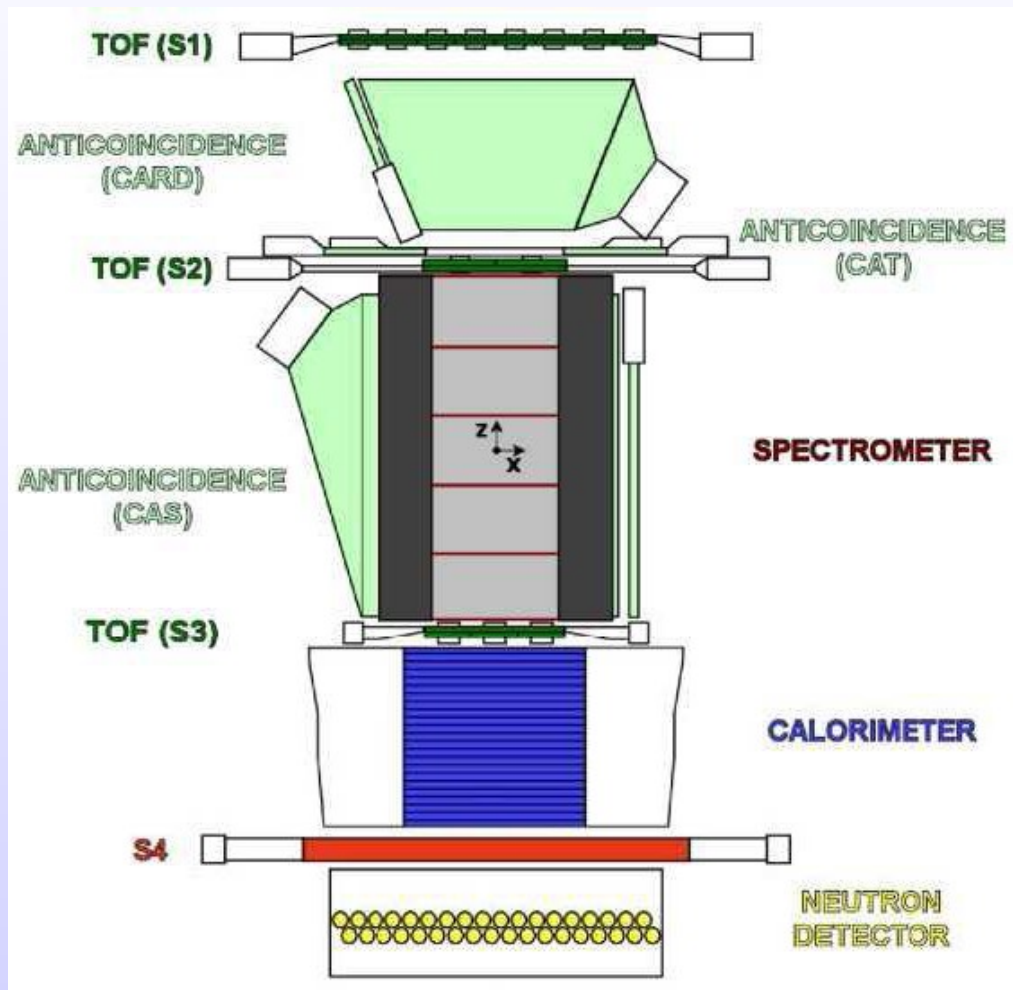


P. Picozza et al., 2007, Astrop. Phys., 27

- height of ~ 1.3 m
- mass of 470 kg
- power consumption of 355 W
- time-of-flight system
- magnetic spectrometer
- electromagnetic calorimeter
- neutron detector
- anticoincidence system
- geometrical acceptance $21.5 \text{ cm}^2 \text{ sr}$
 - determined by the geometry of the spectrometer cavity



The PAMELA experiment

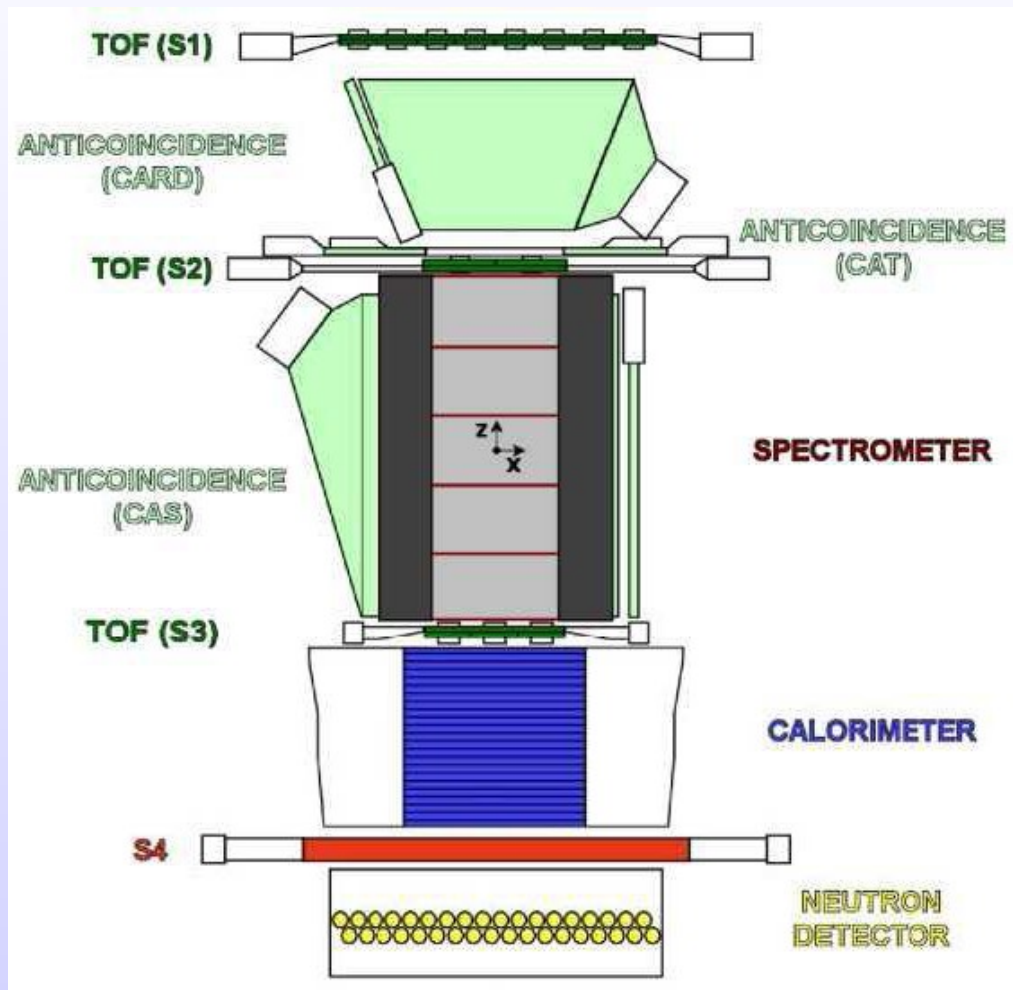


P. Picozza et al., 2007, Astrop. Phys., 27

- **time-of-flight system**
 - 3 scintillator layers
 - dE/dx , charge z
 - flight time, velocity β
 - time resolution ~ 250 ps
 - lepton – hadron separation
 - up to ~ 1 GeV/c
- **magnetic spectrometer**
 - permanent magnet, $B = 0.43$ T along the y -direction
 - 6 silicon detector planes
 - 300 μm thick
 - deflection $\eta = 1 / R$
 - $R = c \cdot p / Z \cdot e$



The PAMELA experiment



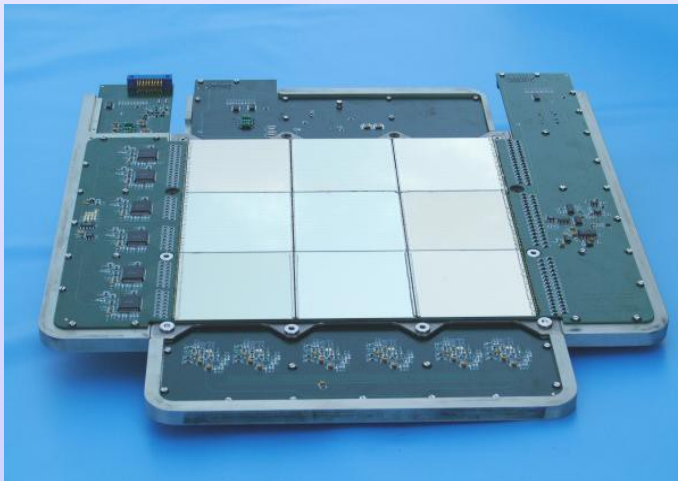
P. Picozza et al., 2007, Astrop. Phys., 27

- **electromagnetic calorimeter**
 - 44 silicon sensor planes (x-y) interleaved with 22 W planes
 - total depth = $16.3 X_0 \sim 0.6 \lambda$
 - lepton – hadron separation
- **neutron detector**
 - 36 counters filled with ^3He in 2 planes
- **anticoincidence system**
 - 4 plastic scintillators (CAS)
 - 1 plastic scintillator (CAT)
 - 4 plastic scintillators (CARD)
 - identify false trigger events



The PAMELA calorimeter

- 44 silicon sensor planes interleaved with 22 plates of tungsten absorbers
- silicon detectors total sensitive area $\sim (24 \times 24) \text{ cm}^2$ arranged in a 3×3 matrix
→ each silicon detector is segmented into 32 strips, 96 strips for each plane
- layout of one plane → Si – X / W / Si – Y
- the total depth is **16.3 X_0** → up to $E \sim 1 \text{ TeV}$ the maximum of the electromagnetic cascade is well contained
- the total depth is \sim **0.6 λ** → $\sim 40\%$ of hadronic particles do not interact

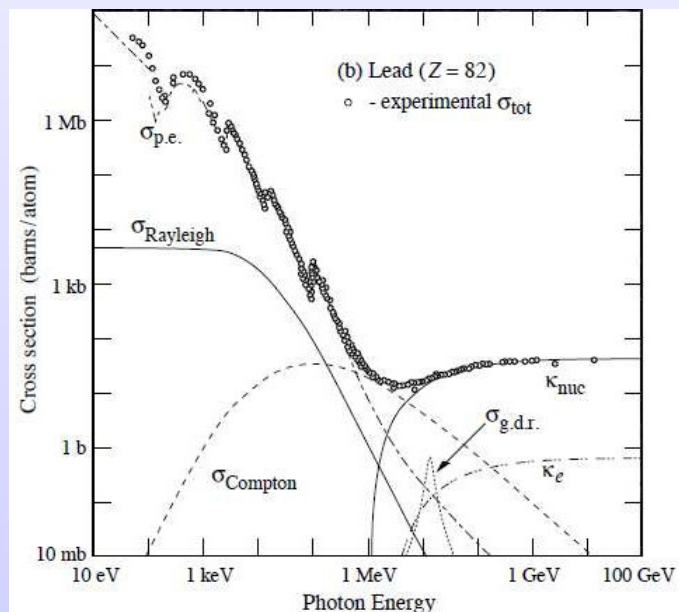


<http://pamela.roma2.infn.it>

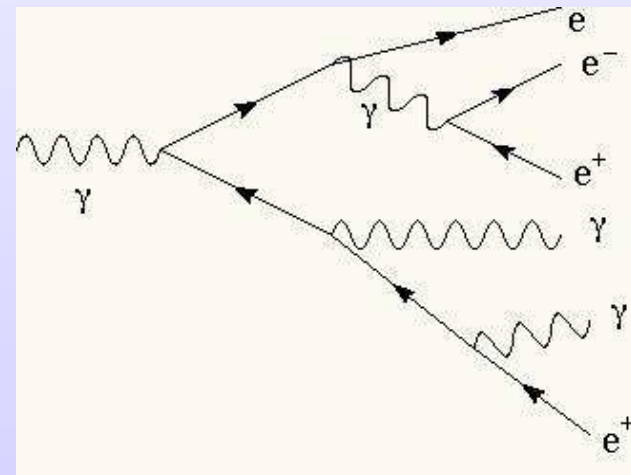


Electromagnetic showers

- Electrons or positrons \rightarrow Ionization, bremsstrahlung
- photons \rightarrow photoelectric effect, Compton scattering, e^\pm pair production
- **radiation length X_0** \rightarrow distance over which an electron or positron loses 63.2% on average of its energy due to bremsstrahlung
- **Molière radius ρ_M** \rightarrow about 90% of the energy is deposited in a cylinder with radius ρ_M around the shower axis

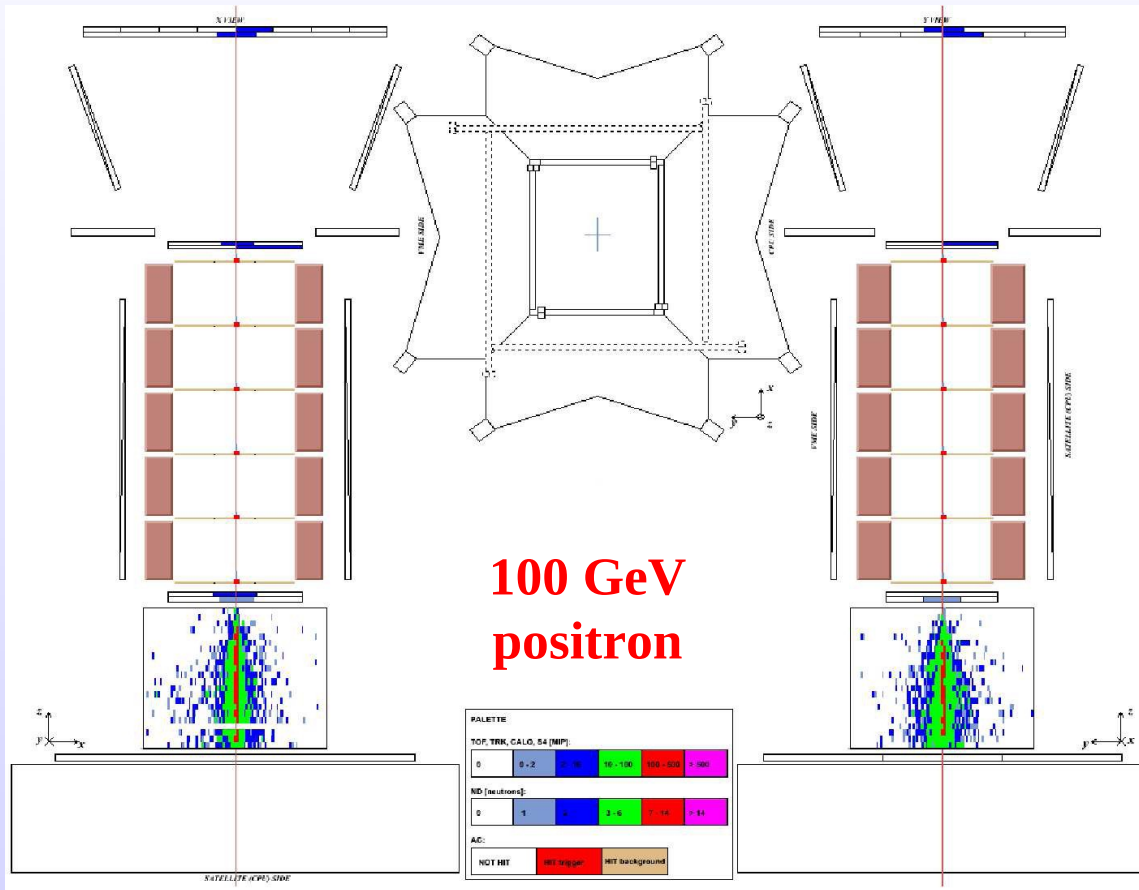


Particle Data Group, 2008





Electromagnetic showers



- **longitudinal profile**
 - governed by the high-energy part of the cascade
 - scales as X_0
- **transverse profile**
 - characterised by a pronounced central core surrounded by a halo
 - described in units of ρ_M

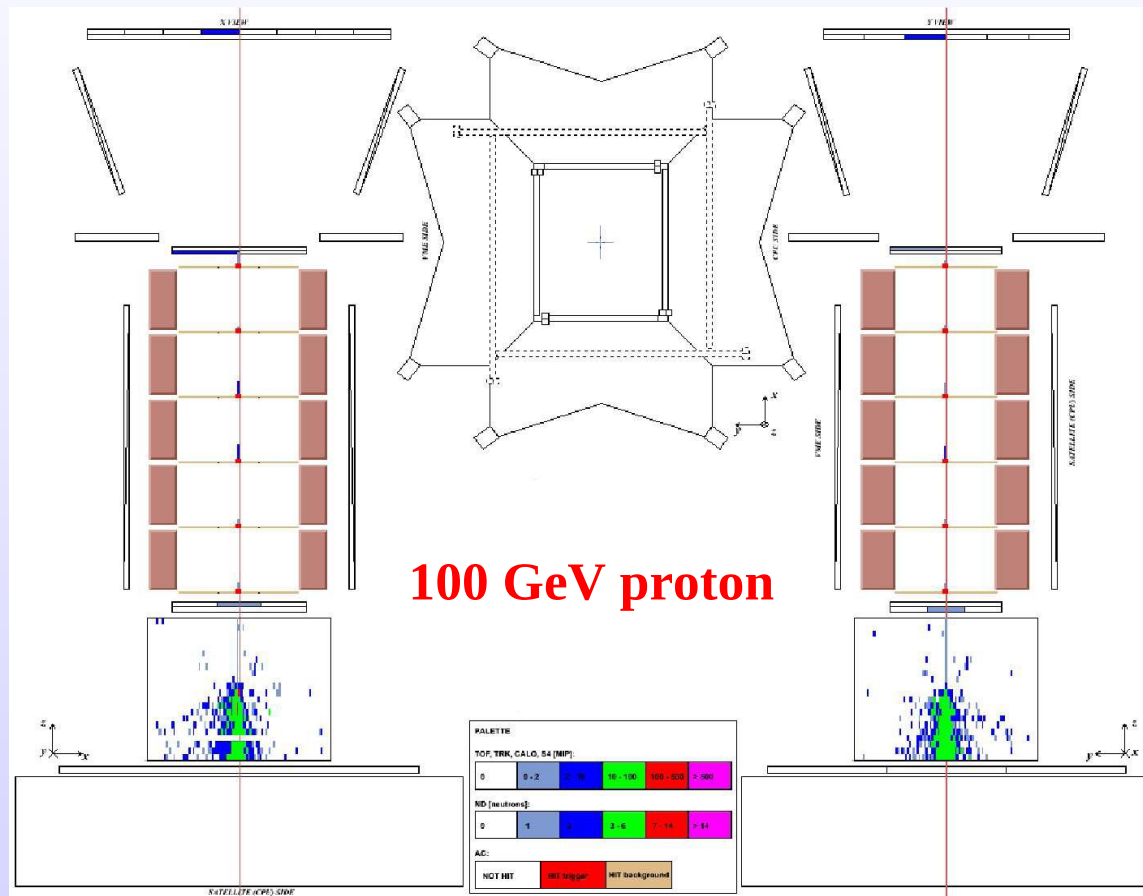


Hadronic showers

- Hadronic interaction \rightarrow strong interactions \rightarrow more complicated shower development compared to the electromagnetic one
- **nuclear interaction length λ_{int}** \rightarrow average distance a hadron has to travel inside an absorber medium before a nuclear interaction occurs
- secondary particles \rightarrow mesons, nucleon, photons
emitted in the forward direction of the primary hadron
- spallation fragments \rightarrow emitted isotropically in the laboratory frame
- \rightarrow longitudinal and transverse profile are very different from those of electromagnetic showers



Hadronic showers



- **longitudinal profile**
 - any maximum lies deeper in the calorimeter for a given incident energy
- **transverse profile**
 - it is broader
 - composed by a narrow core (the electromagnetic component) and a halo (the non-electromagnetic component)



π^0 contamination of hadronic showers

- Hadronic showers generally contain an **electromagnetic** component

$$p + N \rightarrow \pi^+, \pi^-, \pi^0 \quad \pi^0 \rightarrow \gamma + \gamma \rightarrow e^+, e^-, \gamma \dots$$

$$\tau = 8.4 \cdot 10^{-17} \text{ s}$$

probability $\sim 99\%$

- $\sim 1/3$ of the mesons produced in the first interaction are π^0

$$\rightarrow f_{\text{em}} = 1 - (1 - f_{\pi^0})^n$$

n = number of generations

$(1 - f_{\pi^0})^n$ = non-electromagnetic content of the shower

$$f_{\pi^0} \sim 1/3$$

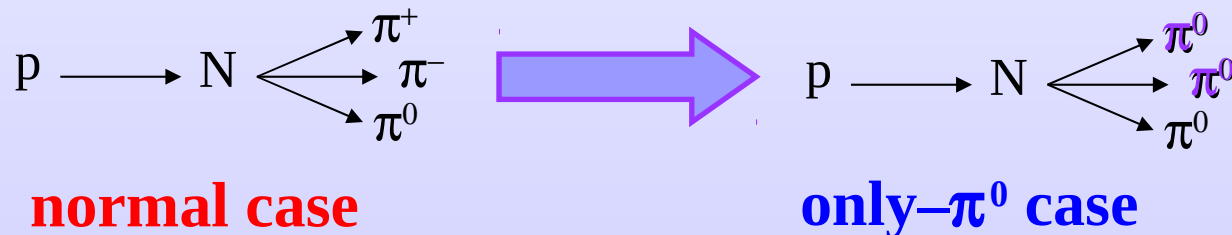
- the electromagnetic contamination of hadronic showers due to π^0 could affect the discrimination between positron and proton events
 \rightarrow it becomes extremely important within the context of the positron analysis



Simulation studies of π^0 contamination

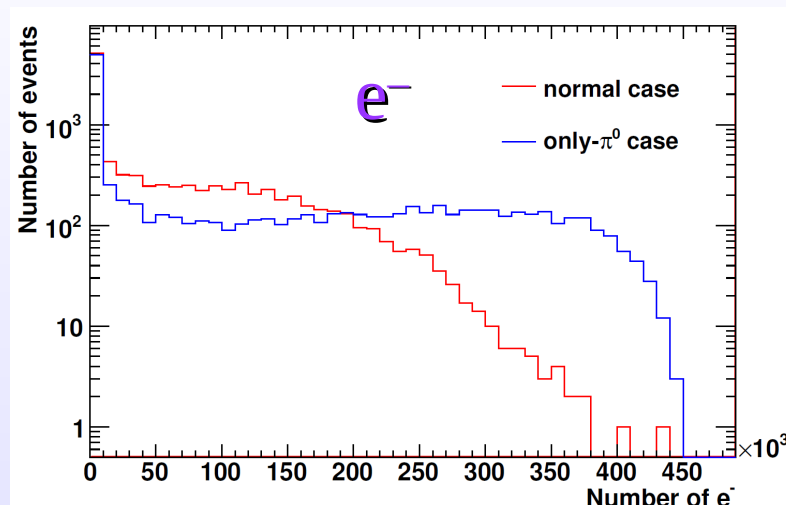
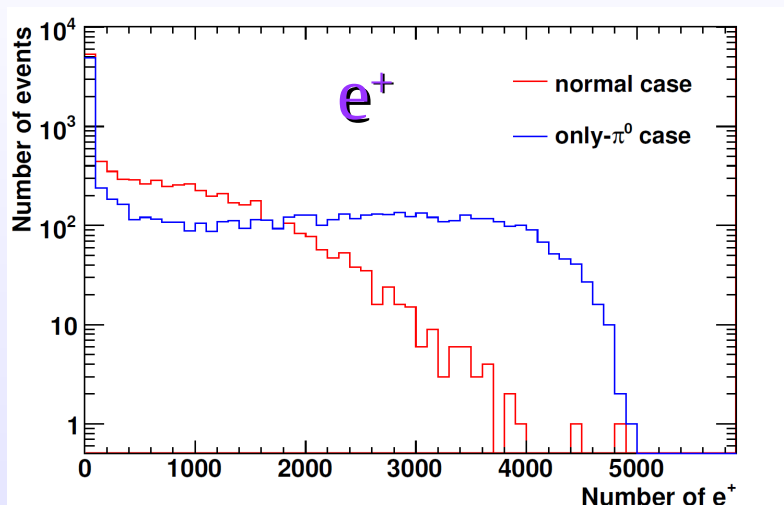
- Study the π^0 produced in hadronic showers within the context of the positron analysis
- Geant3 simulations \rightarrow GPAMELA

\rightarrow in the subroutine GUSTEP **every π^\pm** were changed into **π^0** , in order to increase the production of π^0 (without modifying the cross section of protons!!)

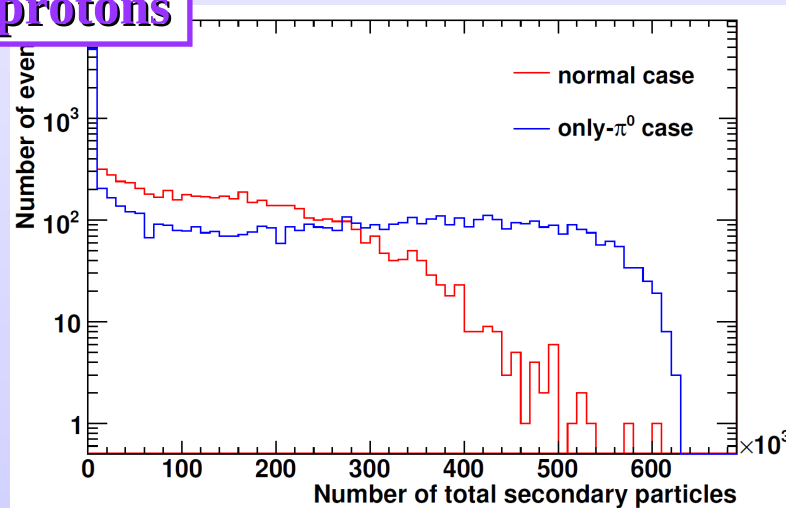
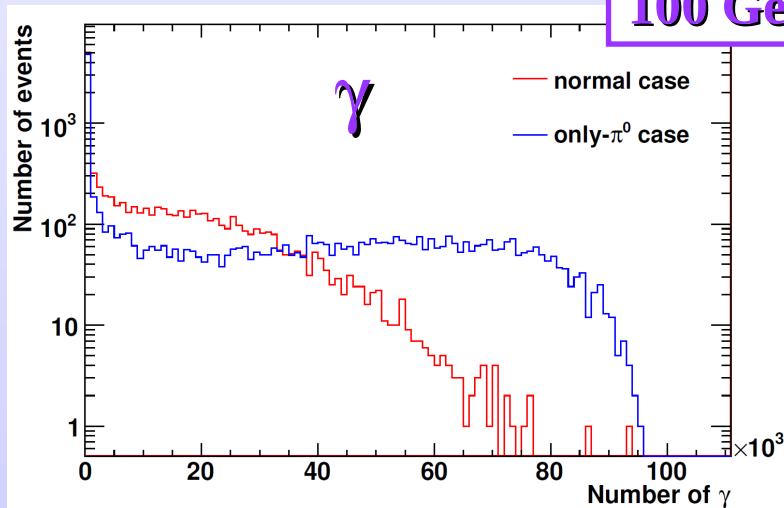




Simulation studies of π^0 contamination



100 GeV protons

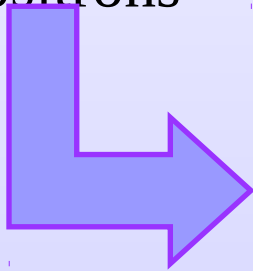




Simulation studies of π^0 contamination

$$E = 20 - 100 \text{ GeV}$$

- 10^5 protons (**normal case**)
- $5 \cdot 10^5$ protons (**only π^0 case**)
- 10^5 positrons

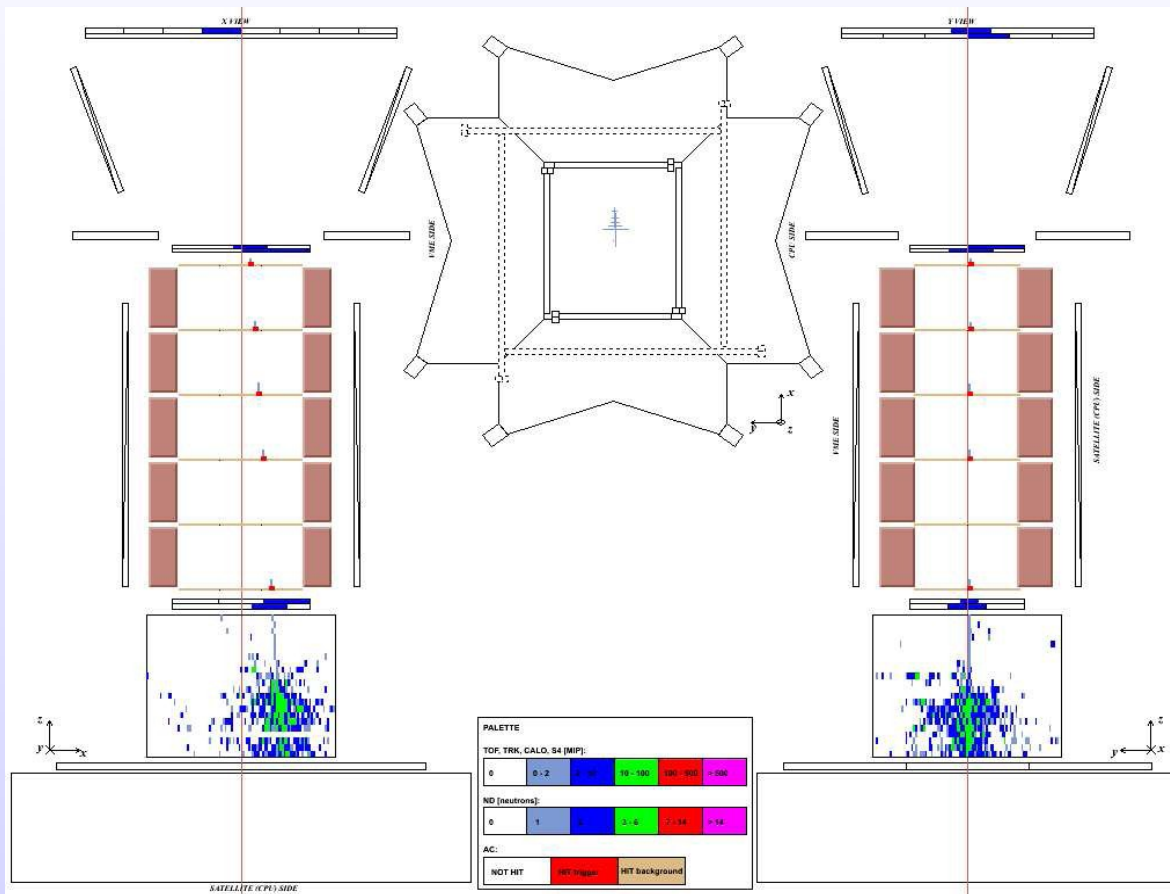


power-law spectrum: $E^{-2.7}$ for protons
 $E^{-3.0}$ for positrons

inclination angle: $\theta = (0 - 20)^\circ$
azimuth angle: $\Phi = (0 - 359)^\circ$



Simulation studies of π^0 contamination

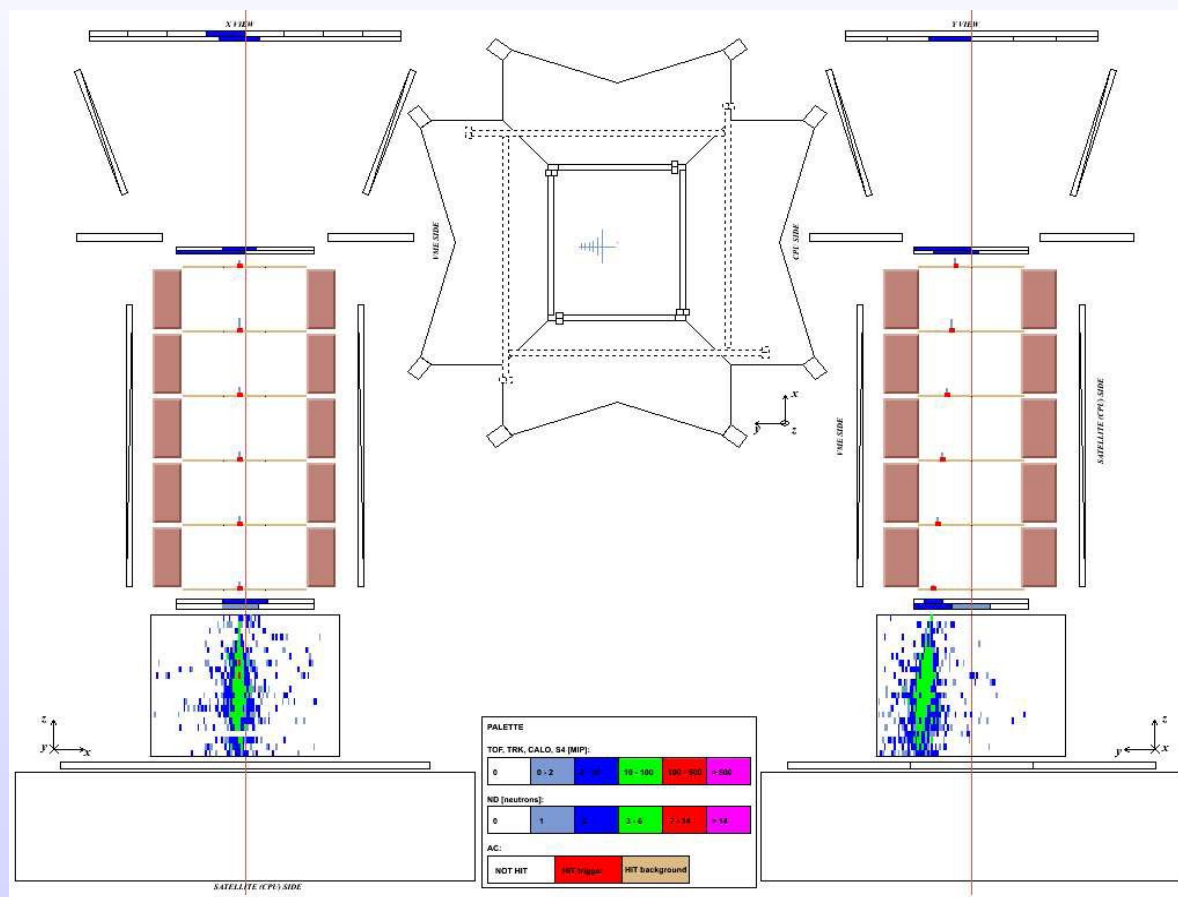


Hadronic shower development
in the **only- π^0** case

- tracker reconstructed rigidity
 $R = 47.6 \text{ GV}$ ($R = c \cdot p / Z \cdot e$)
- the shower development is
similar to an **hadronic cascade**



Simulation studies of π^0 contamination



Hadronic shower development
in the **only- π^0** case

- tracker reconstructed rigidity
 $R = 41.6 \text{ GV}$ ($R = c \cdot p / Z \cdot e$)
- the shower development is
similar to an **electromagnetic
cascade** \rightarrow **problematic!!**

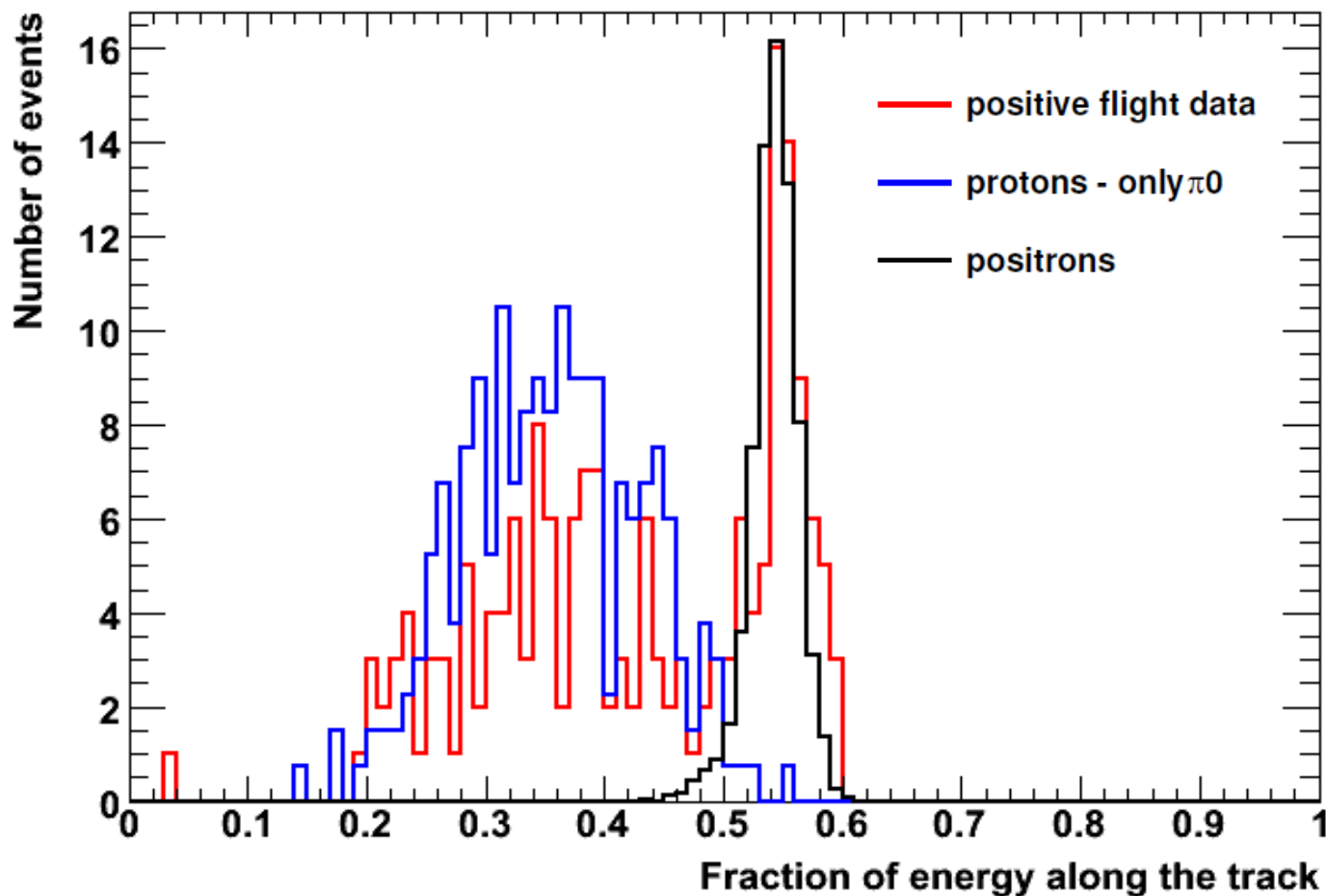


I – The “Nature analysis” approach

- Evaluate the π^0 contamination in positron selection when following the “Nature analysis” approach
- the positron selection cuts used on Nature have been applied to positron and proton simulated samples
- distributions of the energy fraction (q3) have been compared with positively charged particles in flight data in order to investigate the π^0 contamination



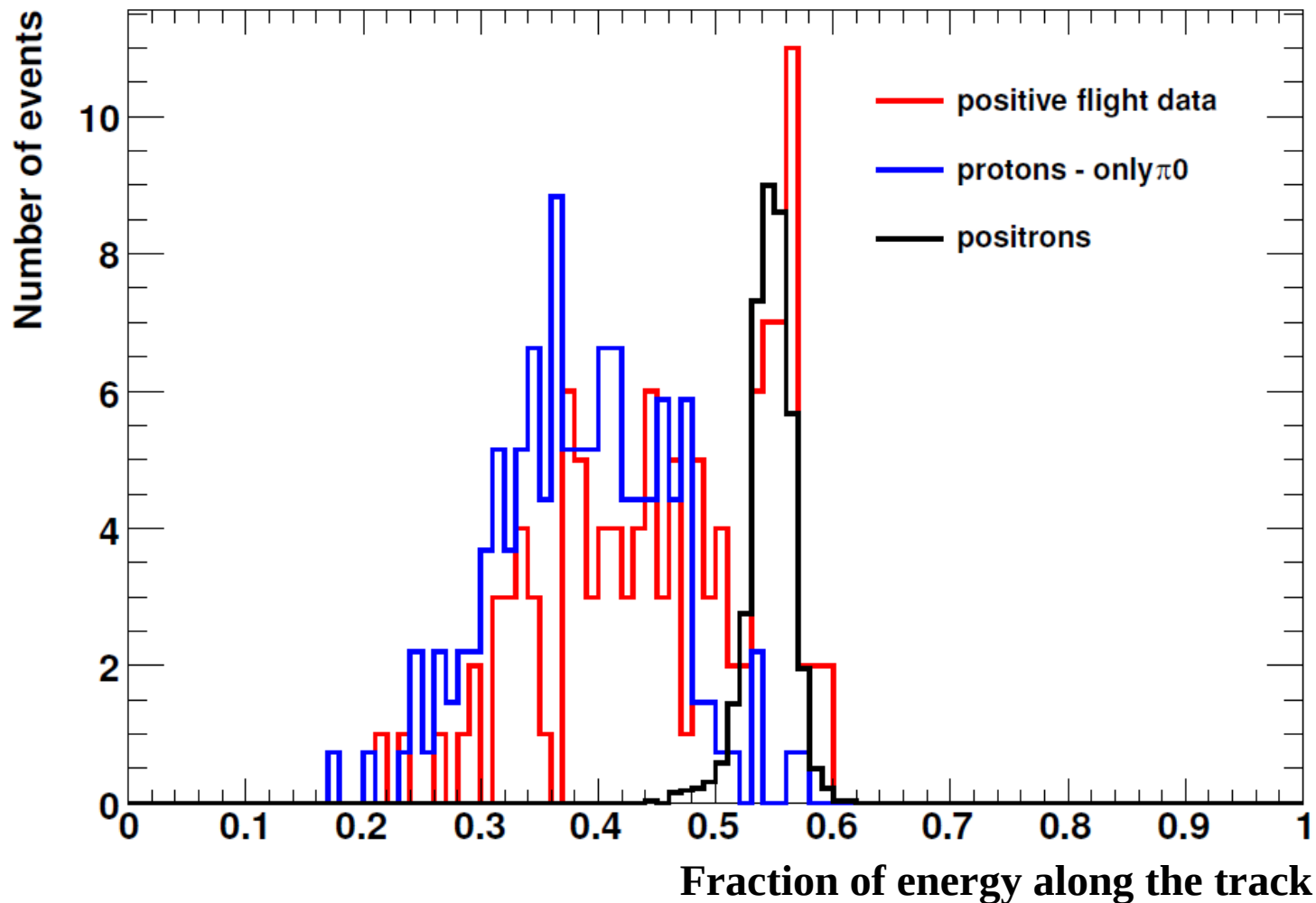
28 – 42 GV



$q_3 \geq 0.5$ selects \rightarrow 3 protons – only- π^0 (simulations)
71 positive flight particles \rightarrow $3/71 = 0.042$



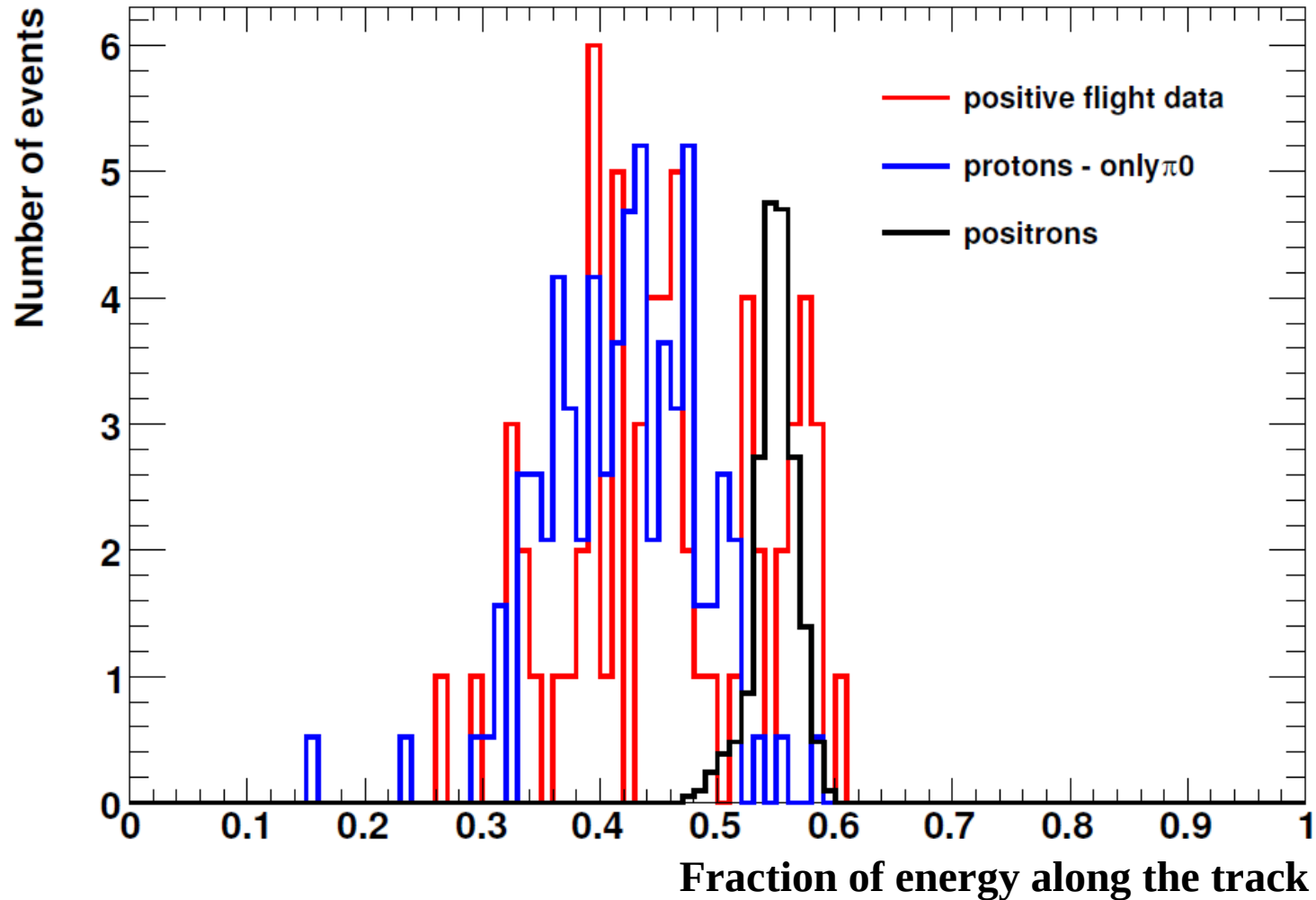
42 – 65 GV



$q_3 \geq 0.52$ selects \rightarrow 4 protons – only- π^0 (simulations)
39 positive flight particles $\rightarrow 4/39 = 0.102$



65 – 100 GV



$q_3 \geq 0.52$ selects \rightarrow 2 protons – only- π^0 (simulations)
19 positive flight particles $\rightarrow 2/19 = 0.105$



I – Positron fraction

Rigidity (GV)	p <i>only</i> - π^0	positive particles	p <i>only</i> - π^0 / positive particles
28 - 42	3^{+5}_{-2}	71	$0.042^{+0.066}_{-0.030}$
42 - 65	4^{+5}_{-3}	39	$0.102^{+0.131}_{-0.067}$
65 - 100	2^{+4}_{-2}	19	$0.105^{+0.226}_{-0.086}$

$q3 \geq 0.5$

$q3 \geq 0.52$

$q3 \geq 0.52$



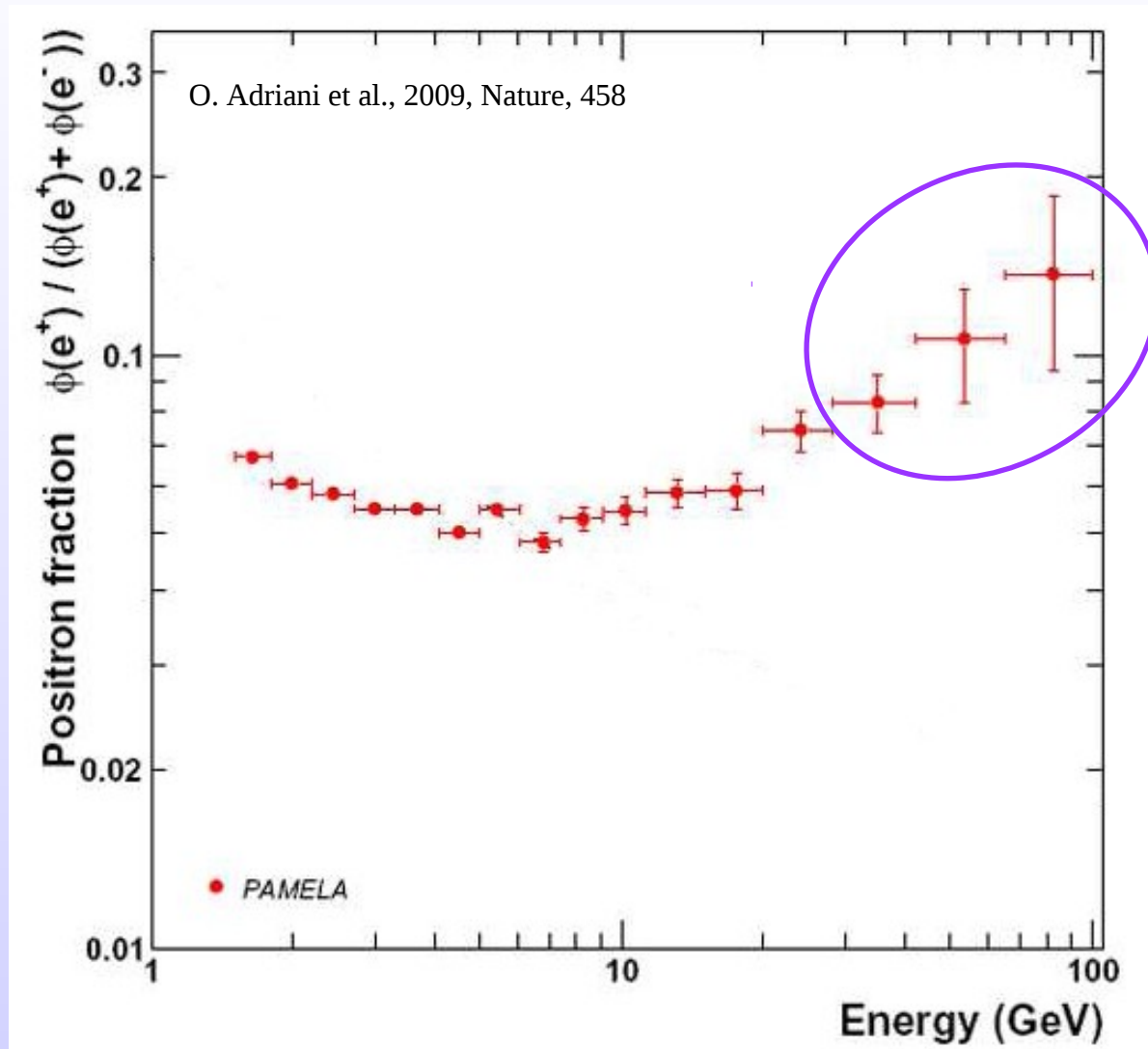
simulations

Nature results

Rigidity (GV)	N_{e+}	N_{e-}	$N_{e+} / (N_{e+} + N_{e-})$	$N_{e+} / (N_{e+} + N_{e-})$
28 - 42	68^{+14}_{-13}	780	$0.080^{+0.016}_{-0.015}$	0.0831 ± 0.0093
42 - 65	35^{+11}_{-10}	292	$0.107^{+0.031}_{-0.029}$	$0.106^{+0.022}_{-0.023}$
65 - 100	17^{+8}_{-7}	101	$0.144^{+0.061}_{-0.054}$	$0.137^{+0.048}_{-0.043}$

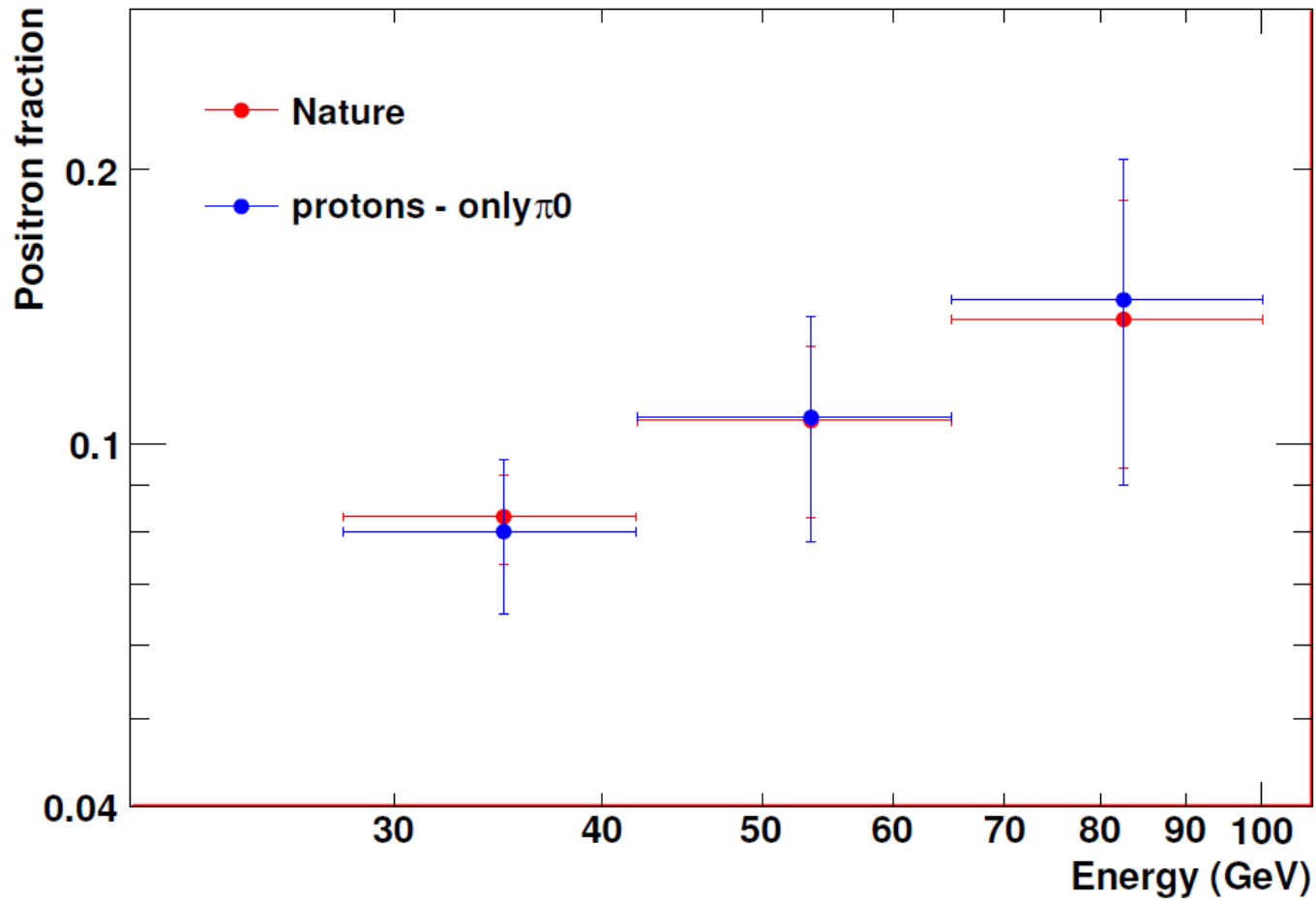


I – Positron fraction





I – Positron fraction





I – Conclusions

- The q_3 distribution of positively charged particles in flight data are well reproduced by two distributions of simulated events:
 - **protons – only- π^0 case** ($q_3 < 0.5$)
 - **positrons** ($q_3 \sim 0.5 - 0.6$)
- no double peak q_3 distribution for simulated protons in the only- π^0 case
- the positron fraction evaluated from proton simulations in the only- π^0 case is compatible with the positron fraction values published in Nature
 - **it is unlikely that the rise in the positron fraction is due to π^0 contamination of hadronic showers**



II – A new approach for positron identification

- π^0 contamination above 100 GeV ???
- study new positron selection cuts using **shower profile variables** in the calorimeter
- standard positron selection cuts have been applied to simulated positron and proton samples in the range **$E = 20 - 100$ GeV**
 - find out what shower profile variables in the calorimeter permit the most efficient positron selection
 - study positron selection efficiency and the related proton contamination



II – Shower profile variables

qtot → total energy deposited in the calorimeter

qtrack → energy deposited in the strips along the track and in the neighbouring strips on each side

qmax → the maximum energy detected in a strip

qcyl → energy deposited in a cylinder of radius 8 strips around the shower axis
($2\rho_M = 8.5$ strips)

qtr → energy deposited in a cylinder of radius 4 strips around the shower axis

qpres → energy deposited in a cylinder of radius 2 strips around the shower axis and only in the first 4 planes of the calorimeter

qtotimp = $qtot / rigidity$

qm = $qmax / qtrack$

q1 = $qcyl / qtot$

q2 = $qtrack / qtr$

q3 = $qtrack / qtot$

qt1 = $qtrack / qcyl$

nstrip → total number of strips hit in the calorimeter

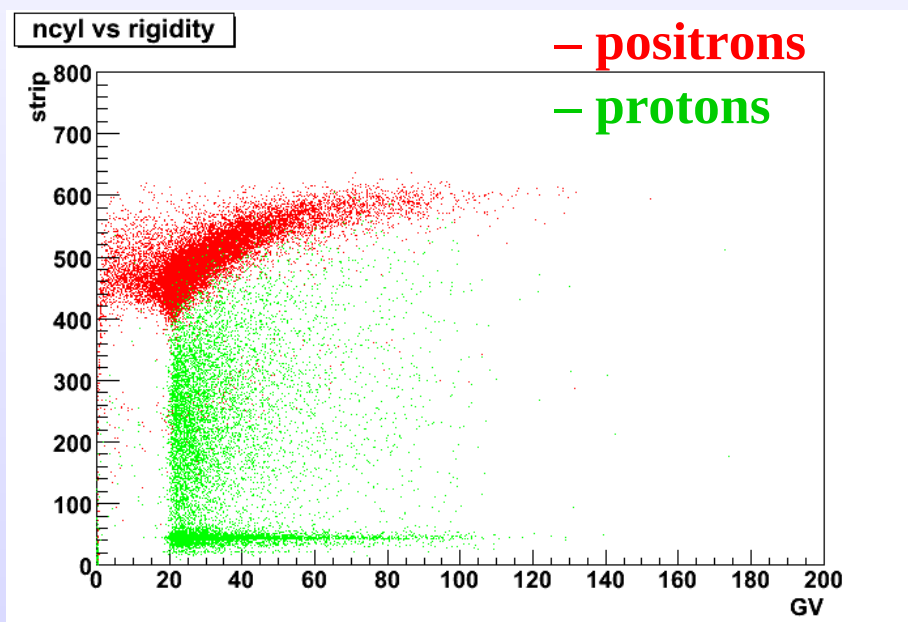
ncyl → number of strips hit in a cylinder of radius 8 strips around the shower axis

ncore → number of strips hit in a cylinder of radius $2\rho_M$ around the shower axis and up to the calculated electromagnetic shower maximum

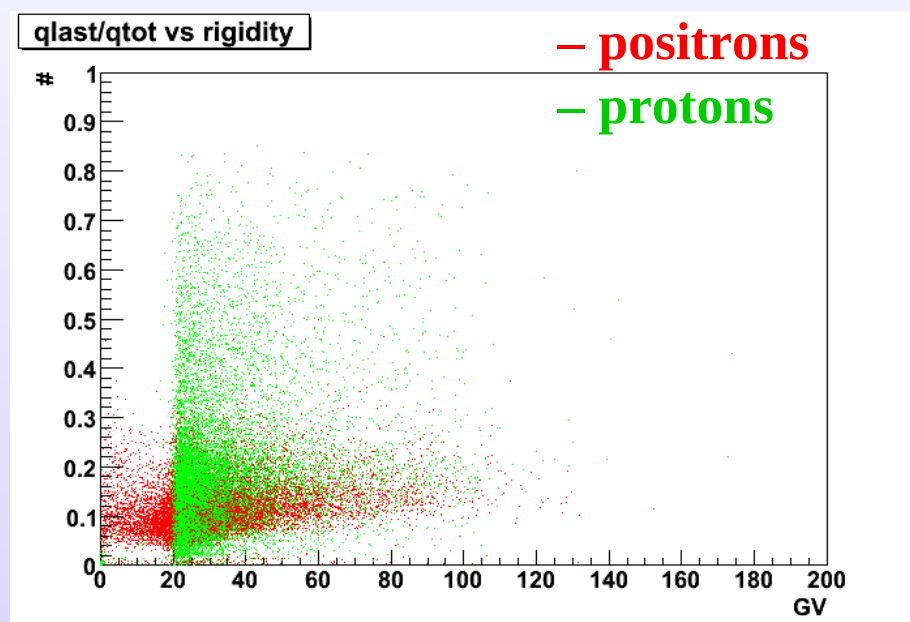


II – A new approach for positron identification

- study distributions of variables as function of the rigidity
 - identify what variables permit an efficient discrimination between positrons and protons



ncyl → number of strips hit in a cylinder of radius 8 strips around the shower axis



qtot → total energy deposited in the calorimeter
qlast → energy deposited in a cylinder of radius 4 strips around the shower axis and only in the last 4 planes of the calorimeter



II – A new approach for positron identification

- study distributions of variables as function of the rigidity
 - identify what variables permit an efficient discrimination between positrons and protons
- construct the variable CALCHI

$$\rightarrow \text{CALCHI} = \sum_i \chi^2_{\text{variable}[i]}$$

$$= \sum_i (\text{variable}[i] - \text{mean}_{\text{variable}[i]})^2 / \sigma^2_{\text{variable}[i]}$$

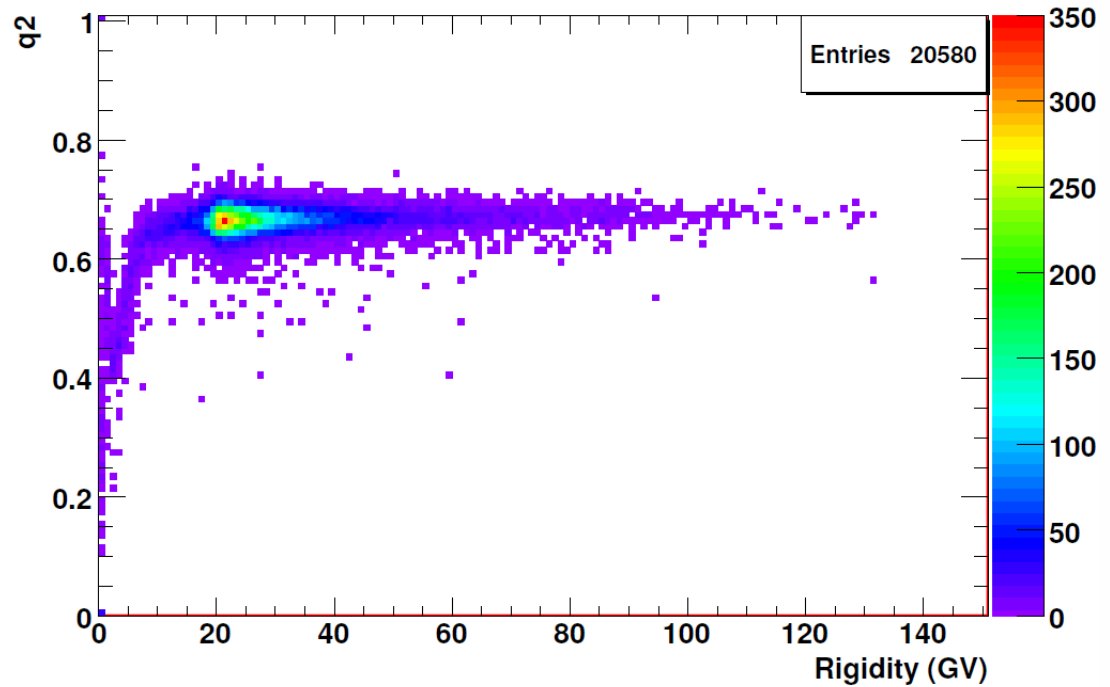
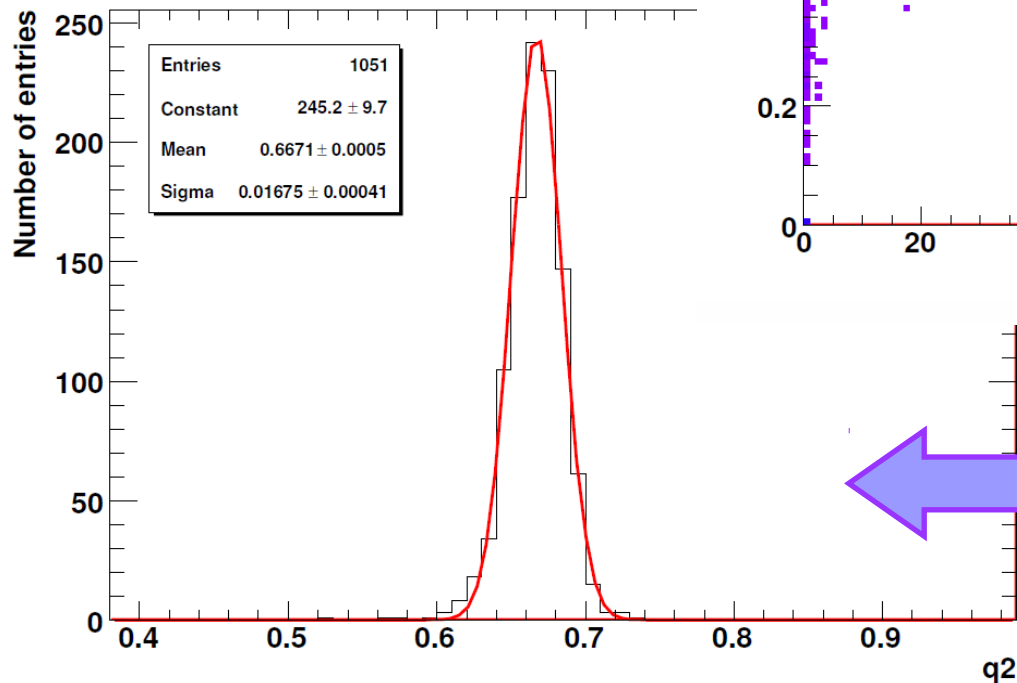
- mean and standard deviation have been tuned on the simulated positron sample



fit of mean and σ distributions as function of the rigidity

20 – 100 GeV

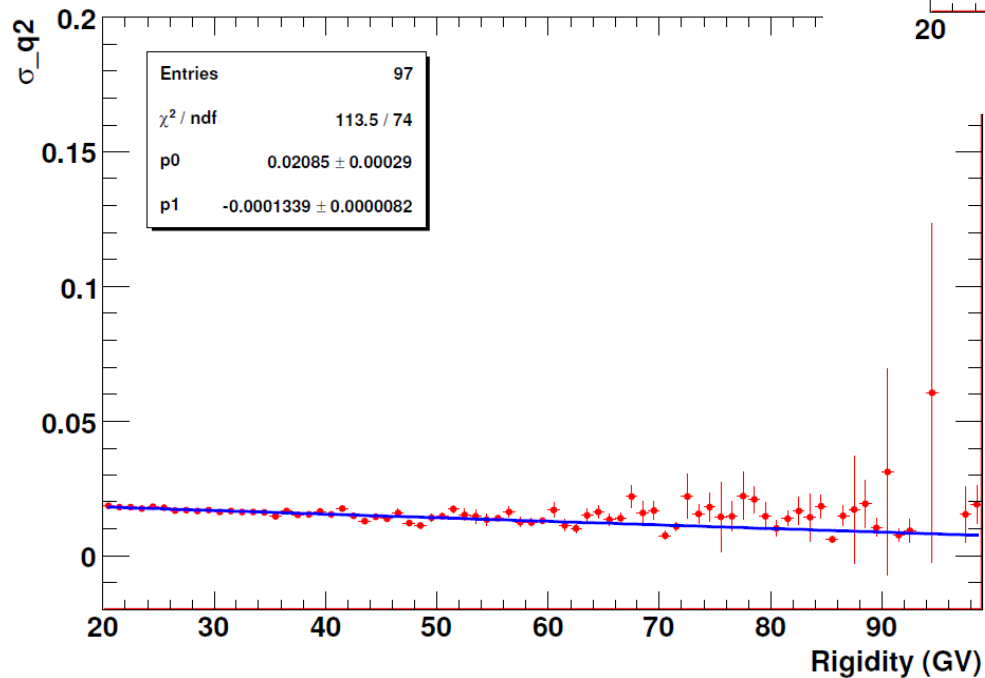
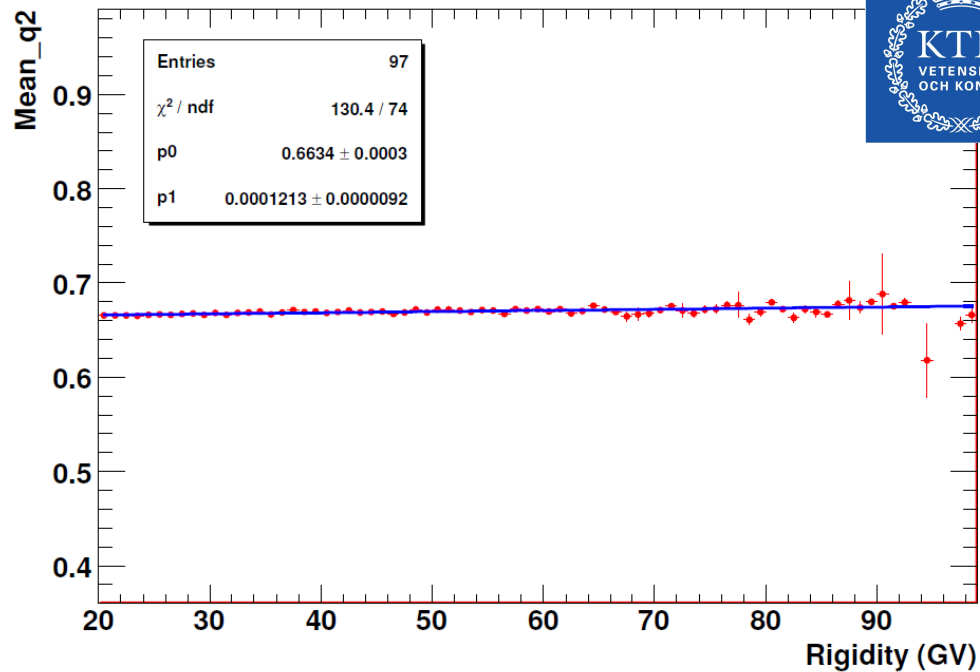
$$q2 = q_{\text{track}} / q_{\text{tr}}$$



$q2$ distribution in the
rigidity bin (30 – 31) GV



20 – 100 GeV



$$\text{mean}_{q2} = 0.6634 + 0.0001213 \cdot R$$

$$\sigma_{q2} = 0.02085 - 0.0001339 \cdot R$$



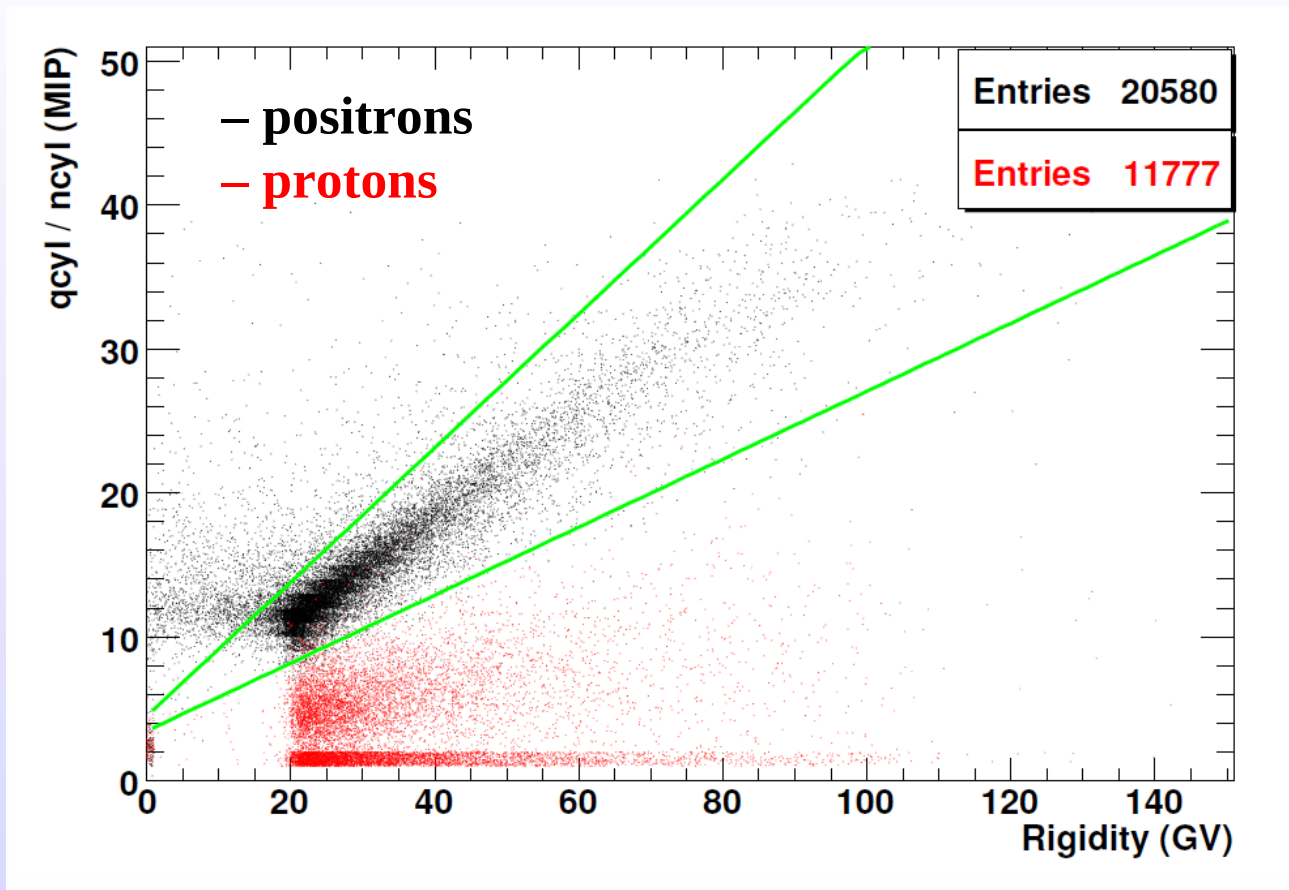
II – Positron selection efficiency study

Selections related to the transverse shower profile variables:

- $\text{mean}_{\text{ncore}} - 3 \cdot \sigma_{\text{ncore}} < \text{ncore} < \text{mean}_{\text{ncore}} + 3 \cdot \sigma_{\text{ncore}}$
- $\text{ncyl} > \text{mean}_{\text{ncyl}} - 3 \cdot \sigma_{\text{ncyl}}$
- $\text{mean}_{\text{qcyl/ncyl}} - 3 \cdot \sigma_{\text{qcyl/ncyl}} < \text{qcyl/ncyl} < \text{mean}_{\text{qcyl/ncyl}} + 3 \cdot \sigma_{\text{qcyl/ncyl}}$
- $\text{qpresh} > 50$
- $\text{qtot/nstrip} > 6$
- $\text{CALCHI} < \text{CALCHI}_{\text{cut}}$



II – Positron selection efficiency study



$$\text{mean}_{q_{cyl}/n_{cyl}} - 3 \cdot \sigma_{q_{cyl}/n_{cyl}} < q_{cyl}/n_{cyl} < \text{mean}_{q_{cyl}/n_{cyl}} + 3 \cdot \sigma_{q_{cyl}/n_{cyl}}$$



II – Positron selection efficiency study

- Many combinations of different shower profile variables have been used in order to obtain the best positron selection efficiency with the smallest proton contamination

$$\text{CALCHI} = \sum_i \chi^2_{\text{variable}[i]}$$

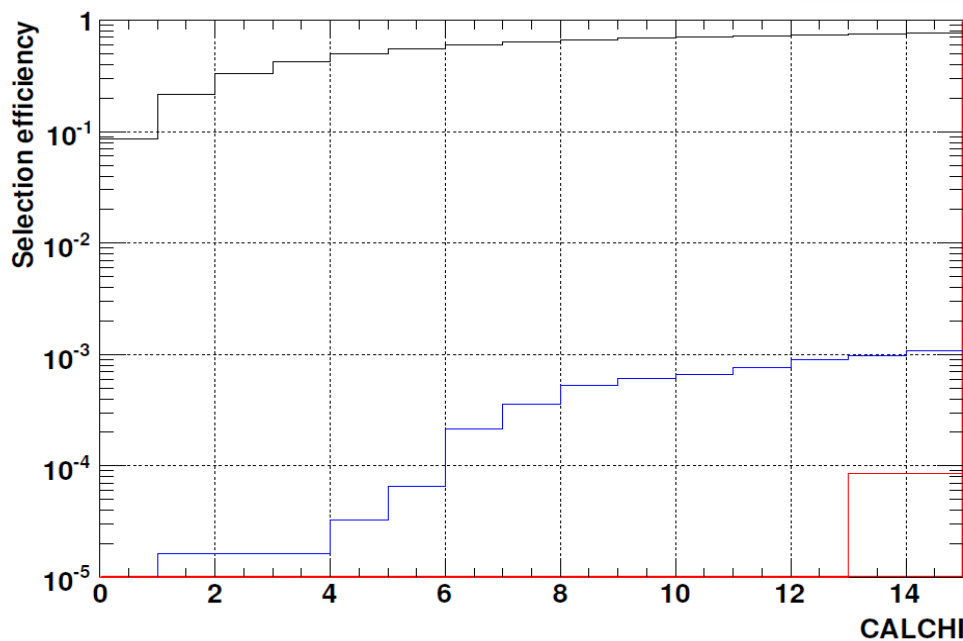
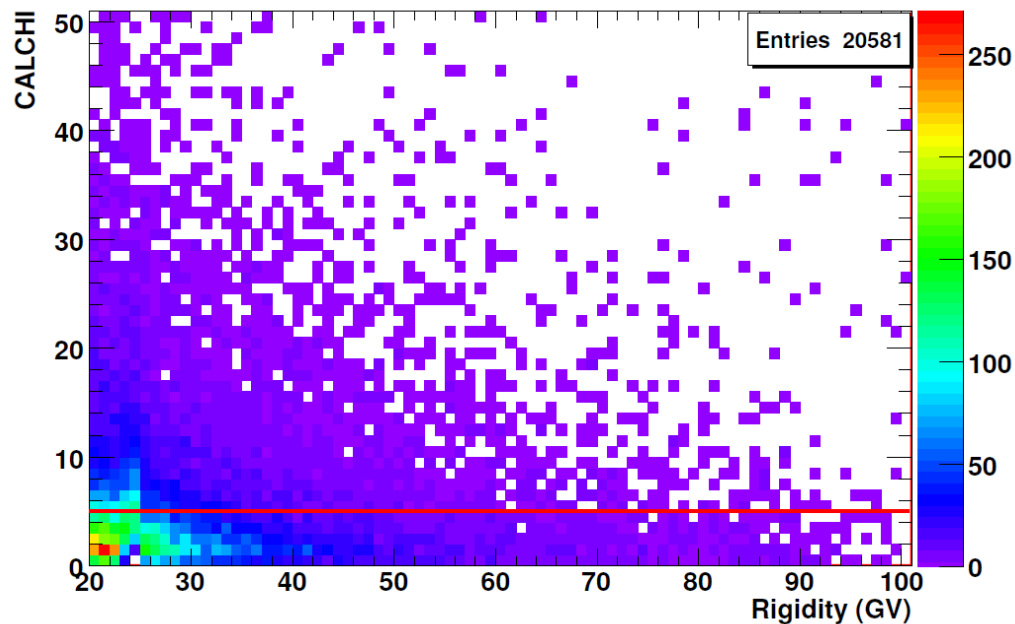
$$= \chi^2_{\text{ncore}} + \chi^2_{\text{q3}} + \chi^2_{\text{qpresh}} + \chi^2_{\text{ncyl}} + \chi^2_{\text{qcyl/ncyl}} + \chi^2_{\text{qtot/nstrip}}$$

- the selection efficiencies were studied for different values of $\text{CALCHI}_{\text{cut}}$



20 – 100 GeV

$\text{CALCHI} < 6$
selects 55.4% of positrons



- positrons
- protons – only- π^0 case
- protons – normal case



II – Positron selection efficiency study

Positron selection efficiencies for different CALCHI values and corresponding proton contamination

<i>Only-π^0 case</i>			
$CALCHI_{cut}$	e^+ efficiency	p efficiency	proton contamination
3	0.328 ± 0.006	$(1.6 \pm_{-1.5}^{6.0}) \cdot 10^{-5}$	$(0.49 \pm_{-0.46}^{1.84}) \cdot 10^{-4}$
4	0.423 ± 0.007	$(1.6 \pm_{-1.5}^{6.0}) \cdot 10^{-5}$	$(0.49 \pm_{-0.46}^{1.84}) \cdot 10^{-4}$
5	0.497 ± 0.008	$(3.3 \pm_{-2.7}^{7.1}) \cdot 10^{-5}$	$(0.66 \pm_{-0.54}^{1.42}) \cdot 10^{-4}$
6	0.554 ± 0.008	$(6.6 \pm_{-4.3}^{8.5}) \cdot 10^{-5}$	$(1.19 \pm_{-0.77}^{1.53}) \cdot 10^{-4}$
7	0.600 ± 0.009	$(2.1 \pm 1.0) \cdot 10^{-4}$	$(3.50 \pm 1.67) \cdot 10^{-4}$
8	0.634 ± 0.009	$(3.6 \pm 1.3) \cdot 10^{-4}$	$(5.68 \pm 2.05) \cdot 10^{-4}$

proton contamination = p efficiency / e^+ efficiency



II – Conclusions

- A new approach based on selections on shower profile variables was studied and tested on **simulations** in the energy range **20 – 100 GeV**
- a combination of six variables permit an efficient positron selection (e.g. **~ 0.50** considering $\text{CALCHI} < 5$)
- these selections yield no proton contamination in the **normal case** sample
- the proton contamination in the **only- π^0 case** sample is of order of **10^{-5}** (considering $\text{CALCHI} < 5$)



Summary

- PAMELA calorimeter → discrimination between electromagnetic and hadronic showers induced by leptons and hadrons
- study the electromagnetic component in hadronic showers produced by π^0 using GEANT3 simulations
 - artificially boosted the number of π^0 produced in hadronic showers (**only- π^0 case** simulations)
- I – the “Nature analysis” approach were applied to simulations
 - the positron fraction is in good agreement with the one published in Nature (O. Adriani et al., 2009, Nature, 458)
 - **it is unlikely that the rise in the positron fraction is due to π^0 contamination of hadronic showers**
- II – a new approach based on selections on shower profile variables was studied and tested on **simulations** in the energy range **20 – 100 GeV**
 - a positron selection efficiency of ~ 0.50 was found with a proton contamination of order of 10^{-5}



Outlook

- Extend the PAMELA positron fraction to $E > 100 \text{ GeV}$
- a new approach, based on selections on shower profile variables, was tested on simulations in the energy range **20 – 100 GeV**
- this new approach will be applied on positive charged particles in flight data
→ **reproduce the positron fraction**
- this method will be studied at **higher energies**, up to $\sim 300 \text{ GeV}$
→ the shower profile variables will be optimised at higher energies
- measurement of the positron fraction for $E > 100 \text{ GeV}$ could solve the problem about primary positron production models



a **P**ayload for **A**ntimatter **M**atter **E**xploration
and **L**ight-nuclei **A**strophysics



Thank you!!!